

Synthesis of Nanomaterials

Mohammad Jafarzadeh
Faculty of Chemistry, Razi University

1. Synthesis Techniques

Top-down methods rely on continuous breakup of bulk matter., starting with a bulk solid and obtaining a nanostructure by structural decomposition.

Bottom-up methods build up nanomaterials from their constituent atoms. Starts with atoms, ions or molecules as “building blocks” and assembles nanoscale clusters or bulk material from them.

Classification of Nanoparticle (NPs) Synthesis Techniques:

- **Solid-State Synthesis of NPs**

- **Vapor-Phase Synthesis of NPs**

1. Inert Gas Condensation
2. Arc Discharge
3. Plasma-Based Synthesis
4. Ion Sputtering
5. Flame-Based Synthesis
6. Pyrolysis/Spray Pyrolysis
7. Laser Ablation

- **Solution Processing of NPs**

1. Sol-Gel Processing
2. Solution Precipitation
3. Micelle and Microemulsion/Water–Oil Microemulsion (Reverse Micelle) Method
4. Solvothermal (Hydrothermal)
5. Sonochemical
6. Microwave-assisted technique
7. Photochemical
8. Electrochemical
9. Liquid-Liquid interface
10. Thermolysis
11. Biological-mediated Method

SOLID-STATE SYNTHESIS OF NANOPARTICLES

In the mid-1990s, Advanced Powder Technology in Australia was pioneer in solid state process. Dry milling was used to induce chemical reactions through ball-powder collisions that resulted in forming NPs.

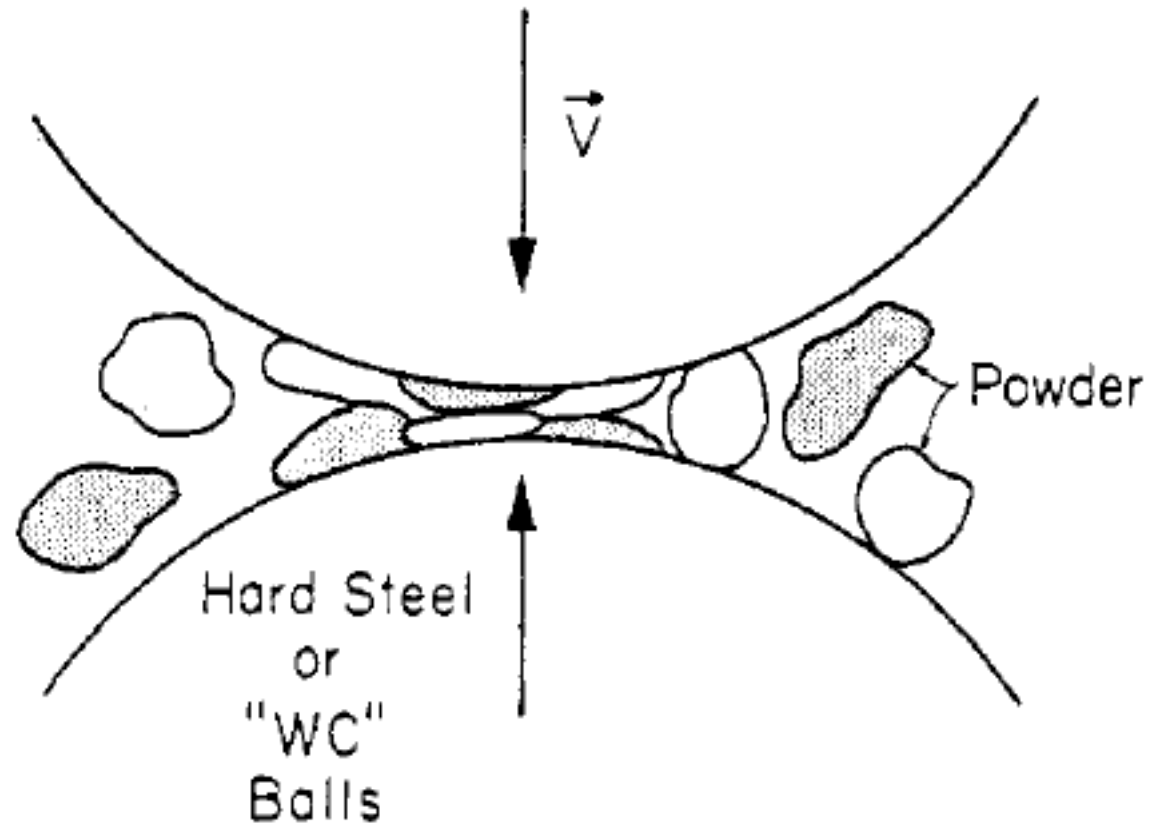
Mechanical attrition or ball milling is used for the formation of nanocrystalline, amorphous, and quasi-crystalline materials in a broad range of alloys, intermetallics, ceramics, and composites.

The ball milling of powders (mechanical attrition) can be divided into two categories:

1. The milling of elemental or compound powders (mechanical milling)
2. The milling of dissimilar powders (mechanical alloying)

A variety of ball mills has been developed for different purposes including tumbler mills, attrition mills, shaker mills, vibratory mills, planetary mills, etc.

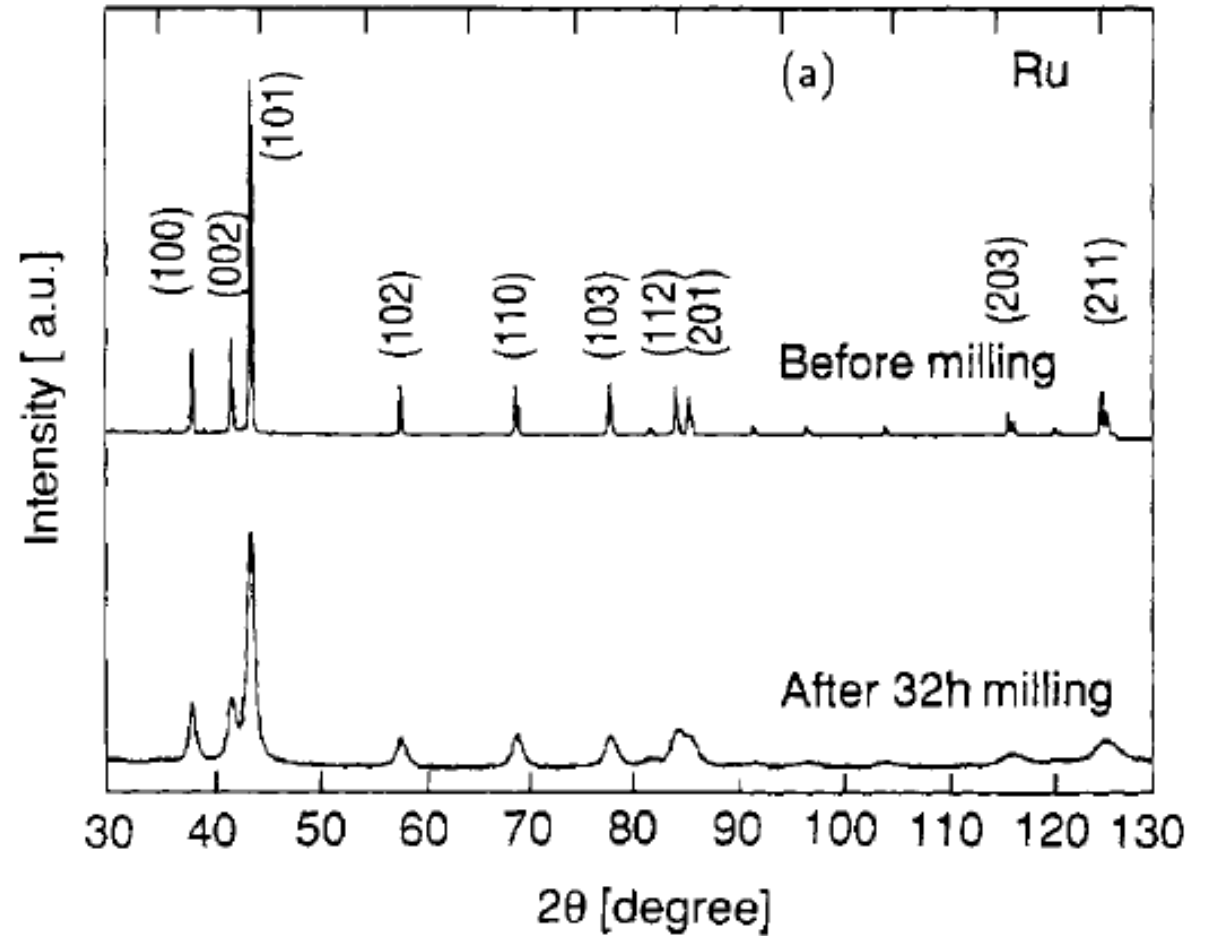
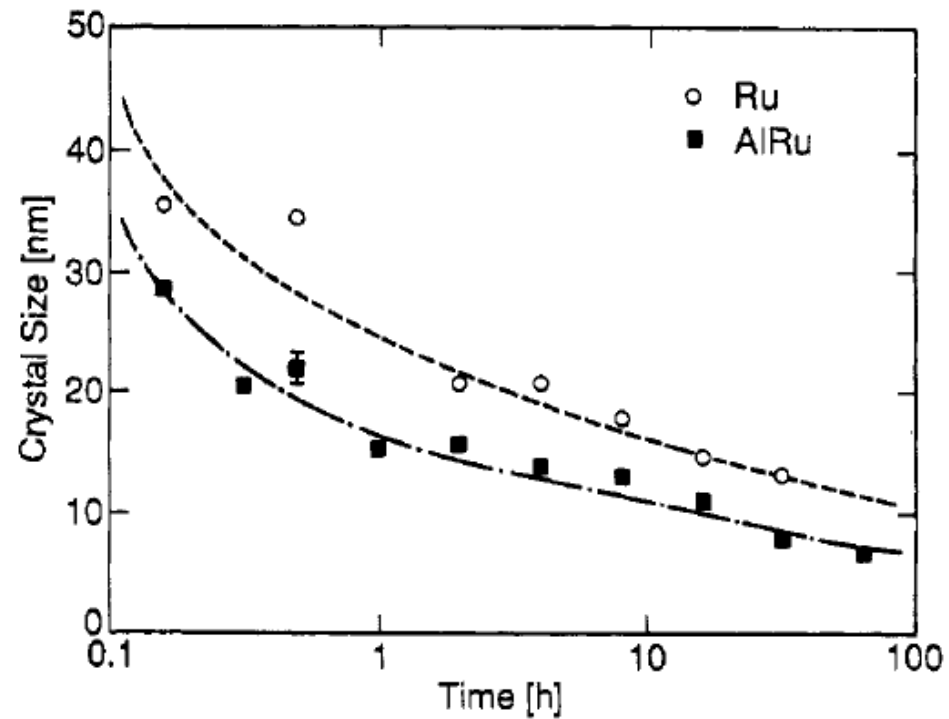
Powders with typical particle diameters of about 50 μm are placed together with a number of hardened steel or tungsten carbide (WC) coated balls in a sealed container which is shaken or violently agitated. The most effective ratio for the ball to powder masses is five to ten.



During mechanical attrition the metal powder particles are subjected to severe mechanical deformation from collisions with the milling tools. Plastic deformation occurs within the particles and the average grain size can be reduced to a few nanometers after extended milling.

The X-ray diffraction patterns exhibit an increasing broadening of the crystalline peaks as a function of milling time.

The domain size (grain or crystal size) is as a function of milling time.



The minimum grain size achieved is dependent: number of process variable & properties of the element or alloy.

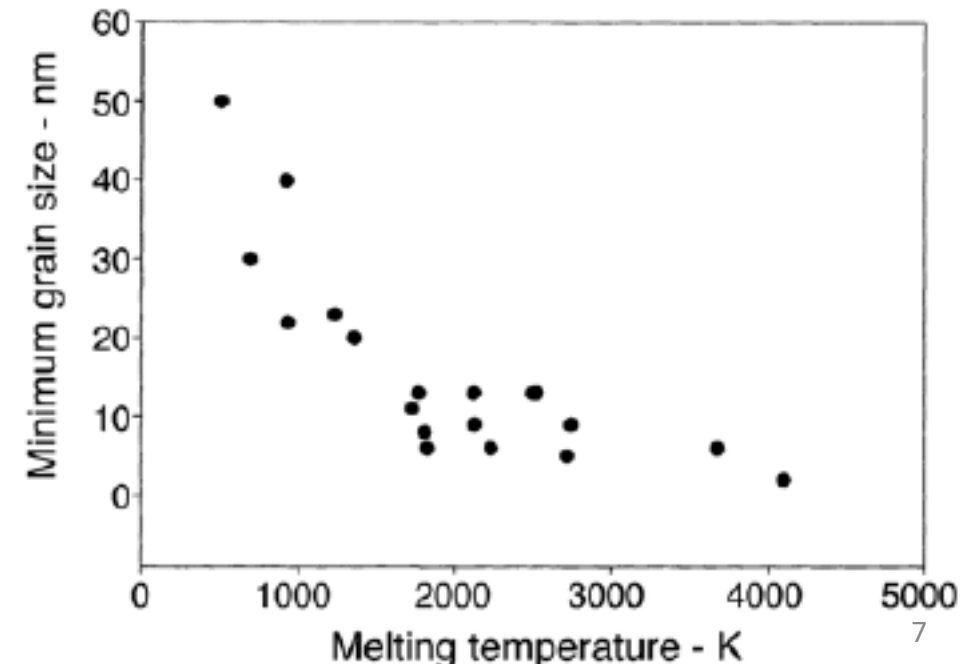
The minimum grain size obtainable, d_{min} , has been attributed to a balance between the defect/dislocation structure (introduced by the plastic deformation of milling) and its recovery by thermal processes.

The energy and frequency of ball-powder-ball collisions determine the final structure.

The minimum grain size induced by milling scales inversely with melting temperature.

Milling temperature affects the rate of nanocrystalline structure develops, smaller grains formed at lower milling temperature.

For Cu: $d = 26$ nm for rt milling and $d = 17$ for milling at -85 oC (cryogenic temperature).



Typical objectives of the milling process include particle size reduction (comminution), solid-state alloying, mixing or blending, and particle shape changes. These industrial processes are mostly restricted to relatively hard, brittle materials which fracture, deform, and cold weld during the milling operation.

Mechanical attrition allows the preparation of alloys and composites which can not be synthesized via conventional casting routes, e.g. uniform dispersions of ceramic particles in a metallic matrix and alloys of metals with quite different melting points (improved strength and corrosion resistance).

Mechanical attrition; as a nonequilibrium process resulting in solid-state alloying beyond the equilibrium solubility limit.

Mechanical attrition offers in preparing nanostructured powders with a number of different types of interface both in terms of structure (crystalline/crystalline, crystalline/amorphous) as well as atomic bonding (metal/metal, metal/semiconductor, metal/ceramic, etc).

Oxide and ferrite compounds can be produced with a spinel structure (e.g., Fe_3O_4 , CoFeO_4) by ball-milling aqueous solutions of metal chlorides and NaOH.

Ball milling of polymeric materials:

In order to fracture the polymer particulate, and on the microscopic level the polymer chains, the milling was conducted at temperature below the glass transition temperature of the given polymer.

Shaw's group has studied a number of homopolymer such as polyamide, polyethylene, acrylonitrile-butadiene-styrene, polypropylene, and polystyrene.

Milling of poly(methyl methacrylate, PMMA) resulted in monotonic decrease in molecular weight and glass transition temperature, reflecting the milling-induced scission of the polymer chain. In some case, the increase in t_g was observed presumably due to a chemical cross-linking in the polymer chain.

The solid-state blending by mechanical attrition of polymeric materials can yield nanoscale dispersions of immiscible polymers.

High-energy ball milling

High-energy milling forces can be obtained by using high frequencies and small amplitudes of vibration.

Shaker mills, which are preferable for small batches of powder ($\sim 10 \text{ cm}^3$, sufficient for research purposes) are highly energetic and reactions can take place faster than with other types of mill.

Since the kinetic energy of the balls is a function of their mass and velocity, dense materials (steel or tungsten carbide) are preferable to ceramic balls.

During the continuous severe plastic deformation associated with mechanical attrition, a continuous refinement of the internal structure of the powder particles to nanometer scales occurs during high energy mechanical attrition.

The temperature rise during this process is modest and is estimated to be 100 to 200 °C.

Proposed mechanism for formation of nanostructures by Ball Milling

Described by Fecht et al.:

Stage 1. Deformation localization in shear bands containing a high dislocation density.

Stage 2. Dislocation annihilation/recombination/rearrangement to form cell/subgrain structures with nanoscale dimensions – further milling extends this structure throughout the samples.

Stage 3. The orientation of the grains becomes random (low angle grain boundaries disappear as high angle grain boundaries replace them) by presumably grain boundary rotation/sliding.

Stage 2 might be considered to be a form of self-assembly since the dense dislocation arrays form into subgrain boundaries in order to lower the energy of the system.

The alloy phase which develops between the pure powder components consists of nanocrystalline grain presumably because of the multiple nucleation events and the slow growth which occur at the relatively low temperature (100-200 °C) during milling.

Drawbacks of ball-milling

impurity pick up

lack of control on the particle size distribution

inability to tailor precisely the shape and size of particles in the range of 10 to 30 nm, as well as the surface characteristics

Ball milling contamination from the milling media (balls and vial) or atmosphere (O_2 , N_2).

If steel balls and containers are used, iron contamination can be a problem.

Atmospheric contamination can be minimized or eliminated by sealing the vial with a flexible 'O' ring (leak-free milling vial) after the powder loading in an inert gas glove box, besides minimizing the milling time.

On the other hand, contamination through the milling atmosphere can have a positive impact on the milling conditions if one wants to prepare metal/ceramic nanocomposites with one of the metallic elements being chemically highly reactive with the gas (or fluid) environment.

Atmospheric control can be used to induce chemical reactions between the milled powders and their environment. By a proper choice of a reactive gas atmosphere (O_2 , N_2 , air, etc.) or a milling fluid (organic fluid which also minimizes wear) the metal powder can be intentionally modified to a nanocrystalline metal-ceramic composite.

VAPOR-PHASE SYNTHESIS OF NANOPARTICLES

Many of the physical methods involve the evaporation of a solid material to form a supersaturated vapor from which homogenous nucleation of NPs occurs.

In these methods, the size of the particles is controlled by temporarily inactivating the source of evaporation, or by slowing the rate by introducing gas molecules to collide with the particles.

The growth generally occurs rapidly, from milliseconds to seconds, requiring a precise control over experimental parameters.

Several specialized techniques have been developed in the last few decades and they can be classified on the basis of the energy source and whether they make use of solid or liquid (vapor) precursors.

1. Inert Gas Condensation

This method is most widely used and provides straightforward means to prepare nanosized clusters, specially of metals. A metal foil or ingot is heated in a ceramic crucible placed in a chamber filled with an inert gas, typically a few torr of argon. The metal vapor cools rapidly losing energy on collision with argon atoms, thereby producing NPs.

In brief: a formation of NPs in a gas phase by condensing atoms and molecules in the vapor phase.

A considerable control could be exercised on the particle size, shape, and extent of aggregation if gas condensation processes could be carried out either in a low-pressure environment, or the NPs were quenched rapidly as soon as they were formed.

The NPs (a mean size of 10 nm) were formed when metal atoms effusing from a thermal source rapidly lost their energy by collisions with gas atoms.

A number of metal nanopowders, including Al, Co, Cr, Cu, Fe, Ga, Mg, and Ni, were synthesized by this technique.

A glass cylinder (diameter, 0.34 m; height, 0.45 m) fitted to water-cooled stainless-steel endplates evacuated to a pressure of 2×10^{-6} torr by an oil diffusion pump.

An alumina crucible was slowly heated via radiation from a graphite heater element.

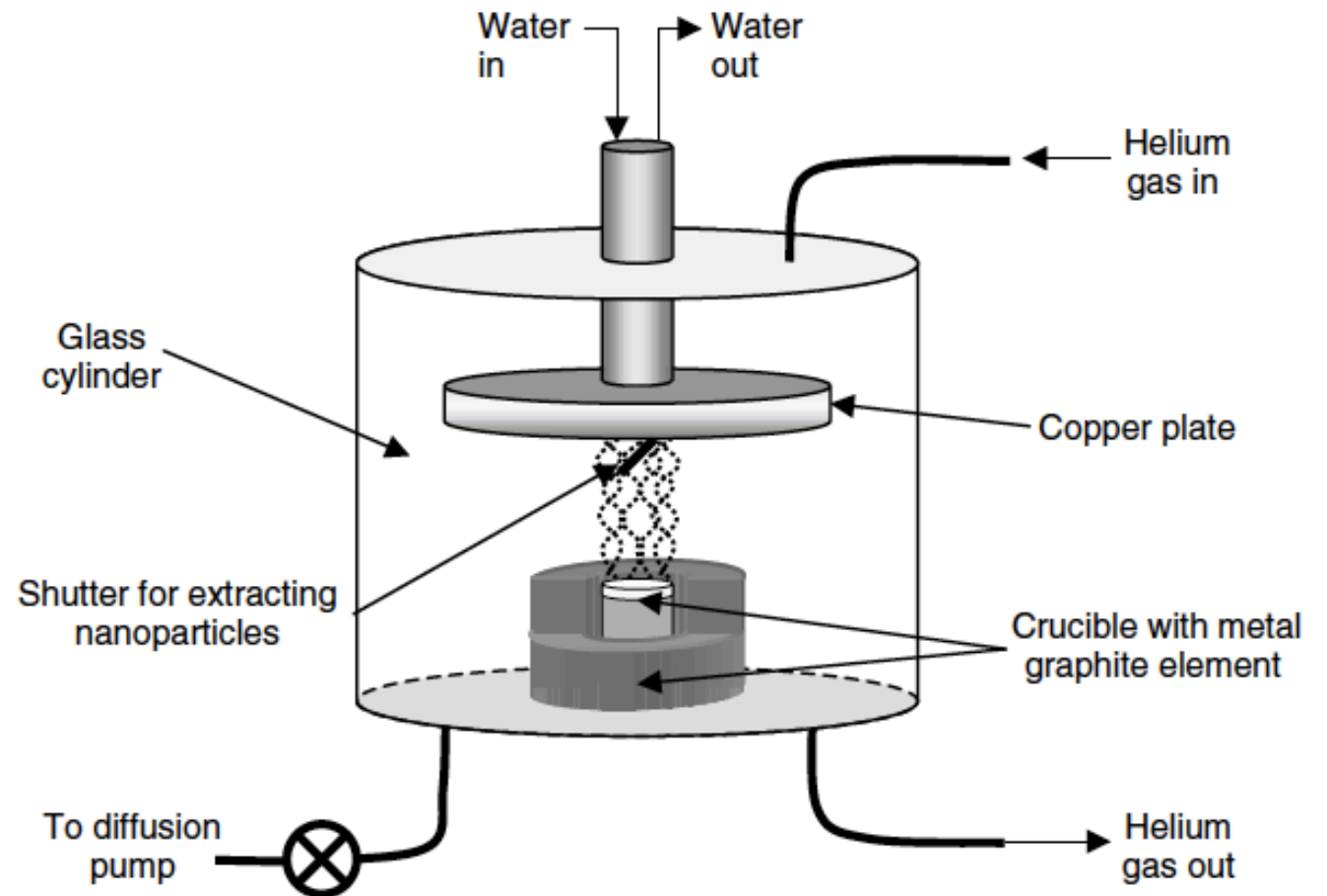
After outgassing the pump line was closed, an inert gas of high-purity argon (0.5 to 4 torr), was introduced into the cylinder.

The crucible was then heated rapidly under quasi-equilibrium conditions (constant temperature and inert-gas pressure).

The NPs, which nucleate and grow in the gas phase, and collected on a water-cooled copper surface.

The short collision mean free path resulted in efficient cooling, producing a high supersaturation of metal vapor, leading to homogeneous nucleation.

The dominant mechanism of particle growth was a coalescence of clusters into NPs.

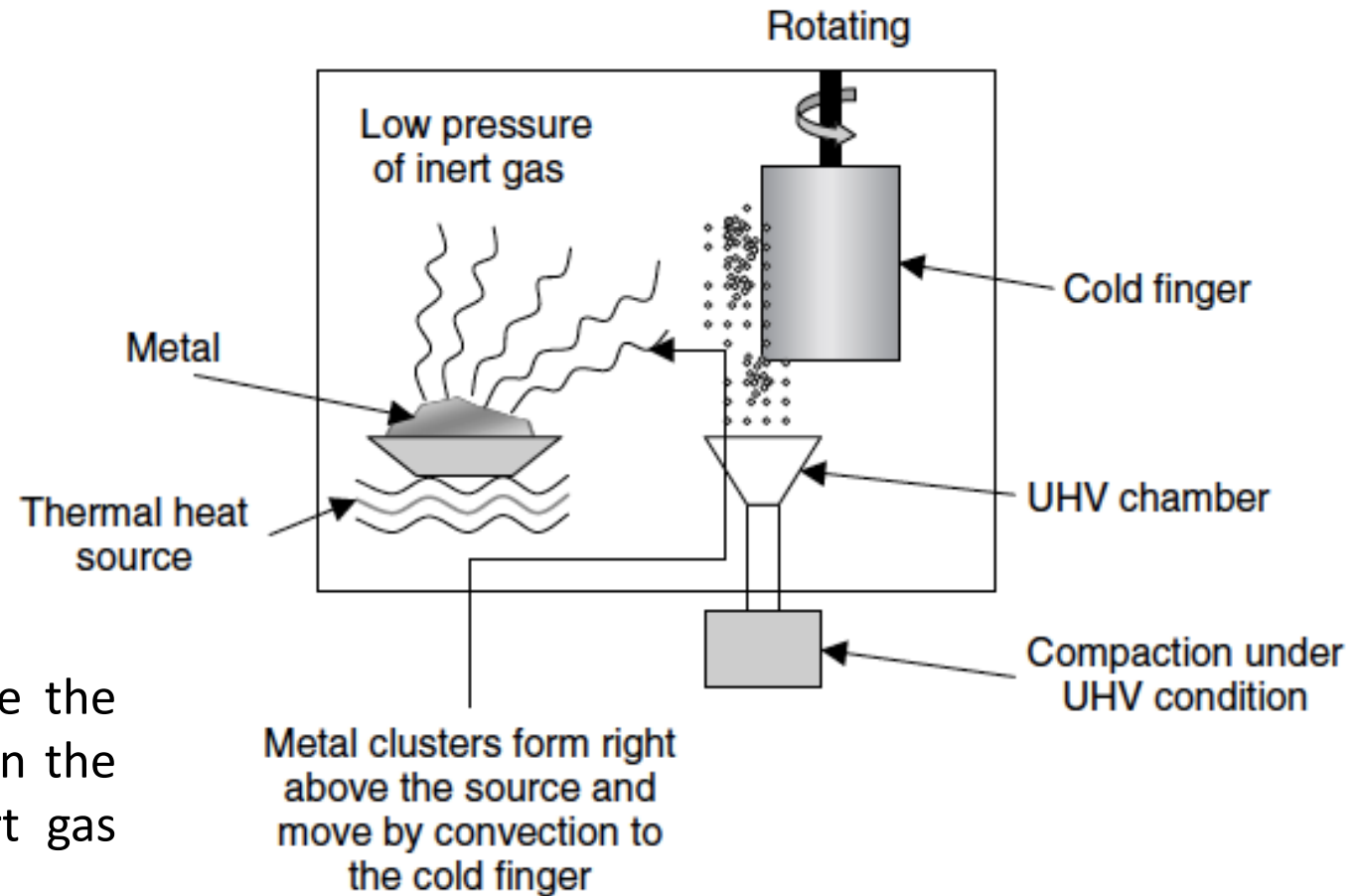


The production rate was about 1 g per run.

Glieter introduced a modification to the process by carrying it out in an ultrahigh vacuum chamber (backfilled with 1 to 10 torr of inert gas) and condensing the NPs on the so-called '**coldfinger**,' which was a liquid-nitrogen-filled rotating cylinder.

NPs develop in a thermalizing zone just above the evaporative source due to interactions between the hot vapor species and the much colder inert gas atoms in the chamber.

The process was versatile as both metals and oxides could be synthesized, the latter being enabled by the introduction of oxygen.



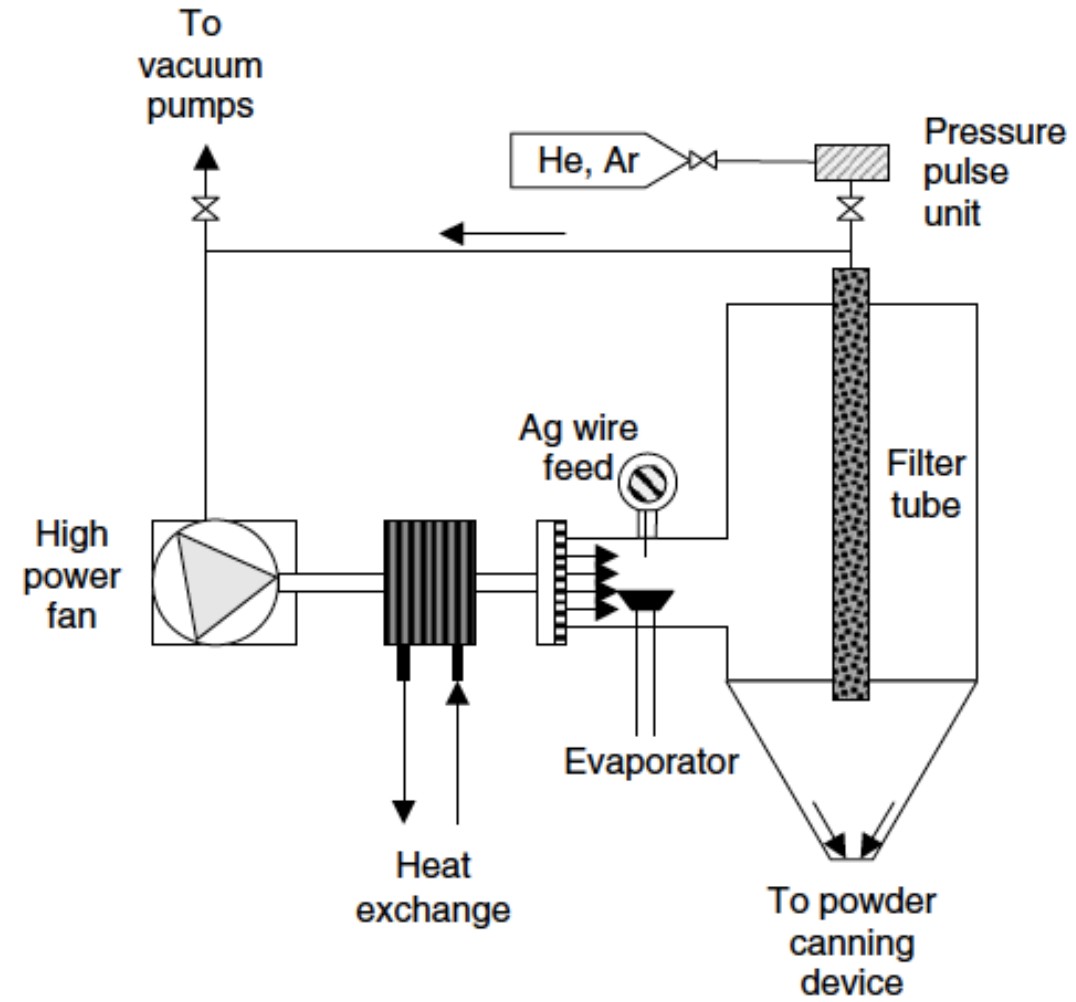
To increase the rate of evaporation of the metal species thereby increasing the production rate, Fraunhofer Institute of Materials developed a closed-loop IGC system.

The system was primarily used for production of silver and copper NPs, but could also be used to produce nanopowders of other elements.

The metal was fed in the form of a wire into a Joule-heated tungsten boat at a background pressure of 2 to 4 kPa.

Filter deposition was used to collect the NPs.

High evaporation rates were sustained by a crossflow of carrier gas.



Lee et al. have prepared SnO NPs under different partial pressures of the convection gases, oxygen and helium.

Semiconductor NPs such as CdS and ZnSe have also been prepared using inert gas condensation.

Gd NPs condensed in an inert gas have been found to exhibit improved stability against oxidation.

In general, gas condensation synthesis is an expensive proposition due to the high-energy cost for evaporating elements and compounds. The only exceptions are those materials that sublime.

Khan et al. have used a sublimation furnace in a controlled environment to vaporize and condense MoO₃ NPs with a high surface area, ~50 m²/g.

2. Arc Discharge

Another means of vaporizing metals is to strike an arc between metal electrodes in the presence of an inert gas.

NPs of metal oxides, carbides, and nitrides can be prepared by carrying out the discharge in a suitable gas medium or by loading the electrodes with suitable precursor.

Balasubramanian et al. prepared cubic AlN particles (15–80 nm) by striking an arc between a W cathode and an Al anode in a gas mixture of nitrogen and argon.

Rexer et al. developed a pulsed arc cluster deposition unit by replacing continuous flow by short gas pulses.

Other related methods include thermal and radio frequency (RF) plasma synthesis. The latter method has been used extensively to produce single crystalline Si NPs. Nanocrystalline ferrite powders (20–30 nm) of Ni–Mn–Fe have also been synthesized using RF plasma torch. Nanopowders of TiO₂ have been prepared by the plasma oxidation of Ti butoxide stabilized with diethanolamine.

3. Plasma-Based Synthesis

A thermal plasma (i.e., ionized gases) is a heat source for melting materials.

Plasma spraying of materials on to substrates to form protective coatings has been a well-established industrial practice for decades. So researchers began using a thermal plasma as a heat source for evaporating materials, both metals and ceramics.

A piece of metal was mounted on a water-cooled copper hearth and heated by a plasma jet flame. The gas atmosphere was helium (a few hundred torr), mixed with about 15% hydrogen. The evolving smoke flowed into a cold cone onto which the ultrafine particles deposited.

Using a 10 kW plasma gun, ultrafine particles of Al, Co, Cu, Fe, Ti, and Ta were produced with the scaled equipment. The mean diameter was ~ 20 nm and the production rate was as high as 50 g/h for some metals.

Problems, such as not being able to focus the plasma at a pressure lower than 200 torr and deterioration of the plasma in long runs, led to curtailment of further development of the process.

Uda at Nisshin Steel Co. developed a direct current arc plasma method to produce metal NPs. A metal block was placed on a water-cooled copper anode plate or a graphite anode crucible. The equipment was evacuated to about 100 Pa and then backfilled with a hydrogen–argon mixture gas at 0.1 MPa pressure, at which point the sample was melted by the arc. Metal vapors were formed and condensed in the gas phase, and subsequently removed by circular gas flow.

Hydrogen gas was reintroduced into the generation chamber by a gas circulation pump. It was found that the presence of hydrogen increased the rate of formation of NPs by a factor of 10 to 10,000 compared to conventional evaporation.

The enhanced evaporation was explained as follows: in arc melting under a hydrogen atmosphere, the molten metal comes into contact with both atomic as well as molecular hydrogen. The former is substantially more soluble in the metal and reaches a supersaturated state rapidly. The extensive dissolution and subsequent evolution of hydrogen gas from the molten metal leads to enhanced evaporation of metal.

Rao et al. argued that the high temperatures in a plasma lead to cold boundary layers and nonuniformities in processing conditions, especially during condensation.

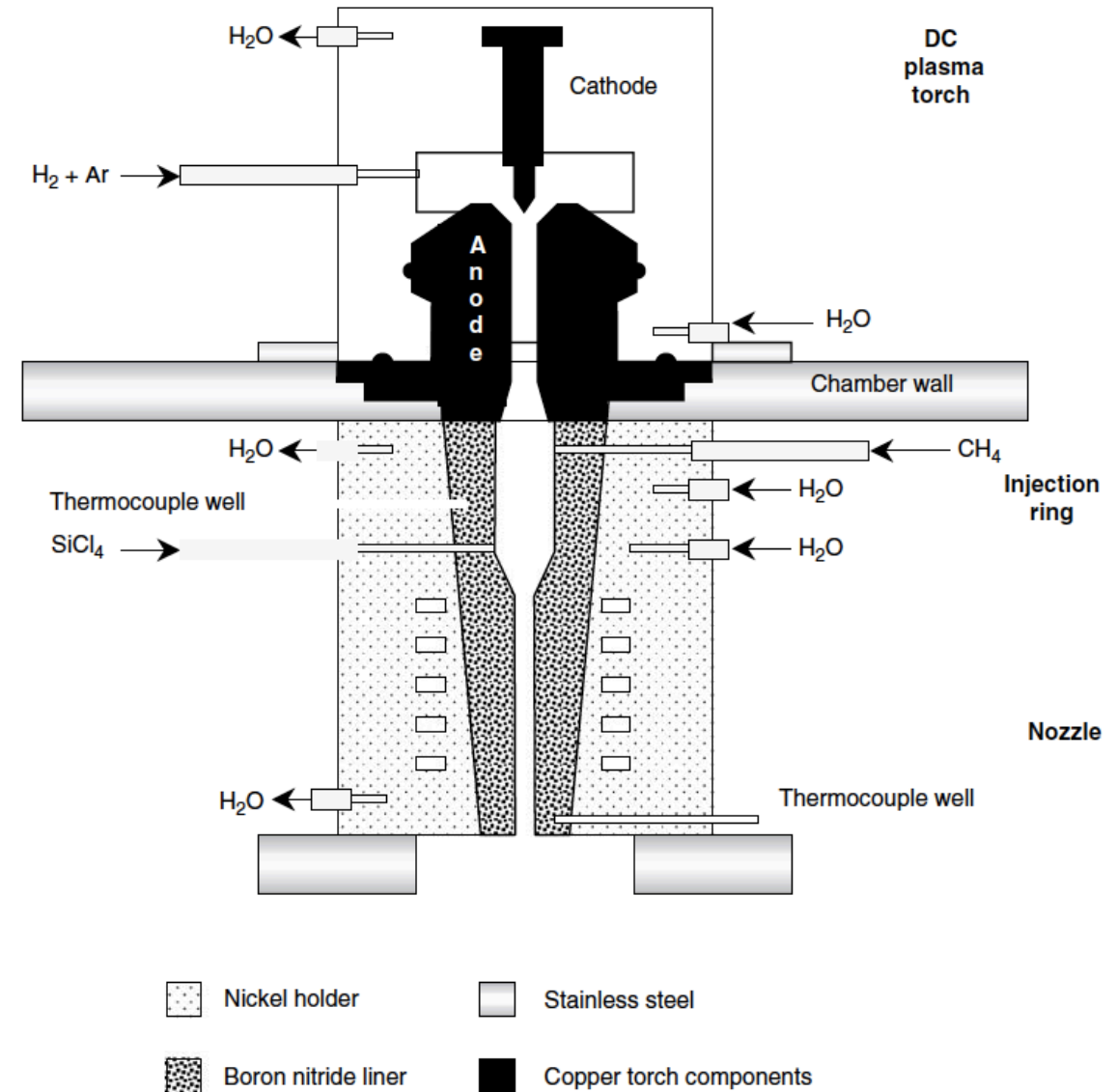
They developed a modified process wherein nonuniformities were minimized by expanding the plasma containing the vapor-phase precursors through a subsonic nozzle with a hot ceramic wall.

This arrangement approached a configuration of 1D flow with 1D temperature gradients in the direction of the flow in the nozzle, leading to high uniformity of the quench rate.

The reactor consisted of a water-cooled chamber with an assembly consisting of a plasma torch, a reactant injection system, and a converging nozzle mounted on the top flange of the chamber.

The torch was a Miller SG- 1B plasma gun with a special tungsten-lined nozzle for argon–hydrogen operation. The 25 mm-long injection section was immediately downstream of the anode, and consisted of a water-cooled nickel ring with a ceramic liner and holes at two axial locations, which are connected to the reactant supplies.

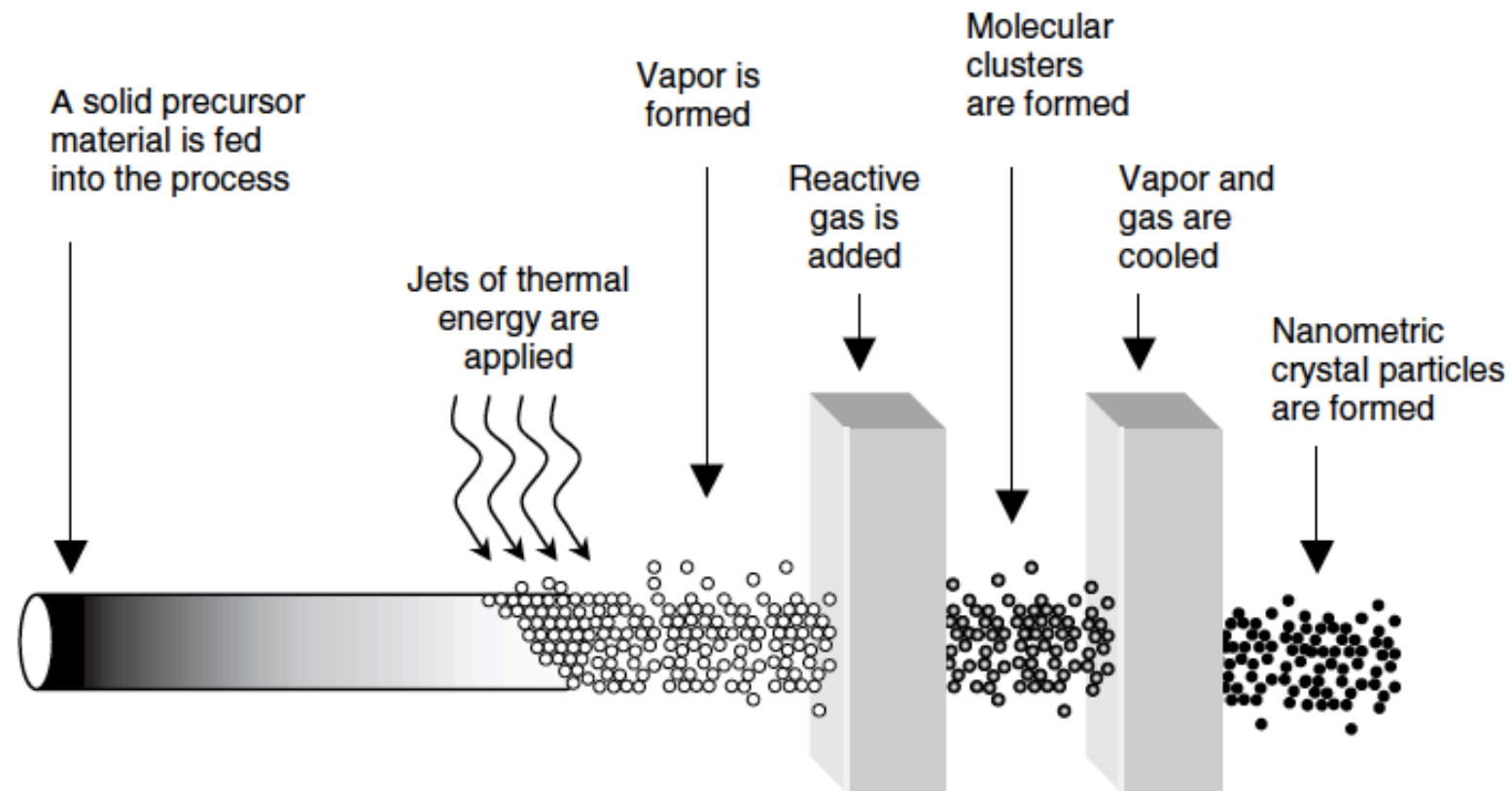
Precursor vapors were introduced through heated lines, and immediately following the injection section is the 50 mm-long converging nozzle held in place by a water-cooled nickel holder. The nozzle and the liner for the injection ring were made of one piece of boron nitride.



A high-purity metal was vaporized and allowed to condense in a chamber via an arc generated by a water-cooled tungsten inert gas torch driven by a power supply.

The working gas then became ionized to a concentration large enough to establish an arc. The interior of the chamber was maintained at a pressure of 250 to 1000 torr.

The consumable precursor material (metal rod with 2 diameter) was fed for continuous production of NPs.



4. Ion Sputtering

In this method, accelerated ions such as Ar^+ are directed toward the surface of a target to eject atoms and small clusters from its surface.

The ions are carried to the substrate under a relatively high pressure (~ 1 mTorr) of an inert gas, causing aggregation of the species.

NPs of metals, alloys, and semiconductors have been prepared using this method.

Urban et al. have demonstrated the formation of NPs of various metals using magnetron sputtering. They formed collimated beams of NPs and deposited them as nanostructured films on Si substrates.

Babonneau et al. obtained spherical and elongated iron NPs buried in carbon matrix.

5. Flame-Based Synthesis

The use of a hydrocarbon (or hydrogen)–oxygen flame to pyrolyze chemical precursor species and produce NPs is attractive in principle due to the fact that flame processes are already in use on a commercial scale.

Over the past decades, research has been directed predominantly toward introducing uniformity and control over the pyrolysis process in a flame, with the anticipation of forming NPs with a narrow size distribution and minimal aggregation.

This included developing flames with a flat geometry, as opposed to the traditional Bunsen burner conical flames.

Pratsinis et al. and Katz and Hung worked extensively on atmospheric flames, including studies on the effect of an electric field on the flame itself as well as on the NPs. This led to an increased understanding of cluster formation and particle growth in a flame.

While the traditional flame processes involved mixing reactants along with the combustibles, a variation of the process was the counter-current flow scheme, in which reactants were fed independently through a separate tube into the flame.

A further variation on the theme of separating the reactant stream from the fuel/oxidizer stream was a multi-element diffusion flame burner.

Wooldridge and co-workers have described one such design, where the flat flame diffusion burner consists of an array of hypodermic needles set in a honeycomb matrix: the fuel is mixed with the precursor reactant and flowed through individually sealed tubes that are less than a millimeter in diameter, and the oxidizer flows through the surrounding channels in the honeycomb.

Modifications continue to be made to developed a five-piped turbulent diffusion flame reactor for producing 50 nm size particles of TiO_2 from TiCl_4 precursor.

Need for a rarefied atmosphere to inhibit collision of hot NPs (cause aggregation) in a flame reactor, Glumac et al. developed low pressure flame synthesis, known as combustion flame-chemical vapor condensation (CF-CVC) process.

The forerunner to the CF-CVC process was the CVC process, which utilized a hot-wall reactor in a low pressure environment.

The processes described above utilized precursor vapors, and so were restricted to oxide ceramics that could be derived from metalorganic or organometallic precursors with ambient pressure boiling points of $\sim 200^{\circ}\text{C}$ or lower. As such, acetates and nitrates were not utilized.

Laine and coworkers atomized nonvolatile precursors dissolved in a solvent and directed them through a combustion flame. Powders with high surface area were formed as a result of rapid pyrolysis.

The range of compositions of nanopowders could now be expanded to multicomponent oxide materials. It should be noted that the mechanism of NP formation is unlike that of vapor condensation when nonvolatile species are pyrolyzed in the flame.

6. Pyrolysis/Spray Pyrolysis of Nanoparticles

In laser pyrolysis, a precursor in the gaseous form is mixed with an inert gas and heated with CO₂ infrared laser (continuous or pulsed), whose energy is either absorbed by the precursor or by an inert photosensitizer such as SF₆.

Swihart, Ledoux et al., and Ehbrecht and Huisken prepared Si NPs by laser pyrolysis of silane. By using a fast-spinning molecular beam chopper, Si NPs in the size range of 2.5–8 nm were deposited on quartz substrates to study quantum confinement effects.

Li et al. improved the stability of the Si NPs (~5 nm) by surface functionalization and obtained persistent bright visible photoluminescence.

Zhao et al. obtained Co NPs by laser pyrolysis of Co₂(CO)₈ vapor at a relatively low temperature of 44 °C. Ethylene was used as a photosensitizer for CO₂ laser emission.

Grimes et al. synthesized single phase ferromagnetic γ -Fe₃N and FeC NPs.

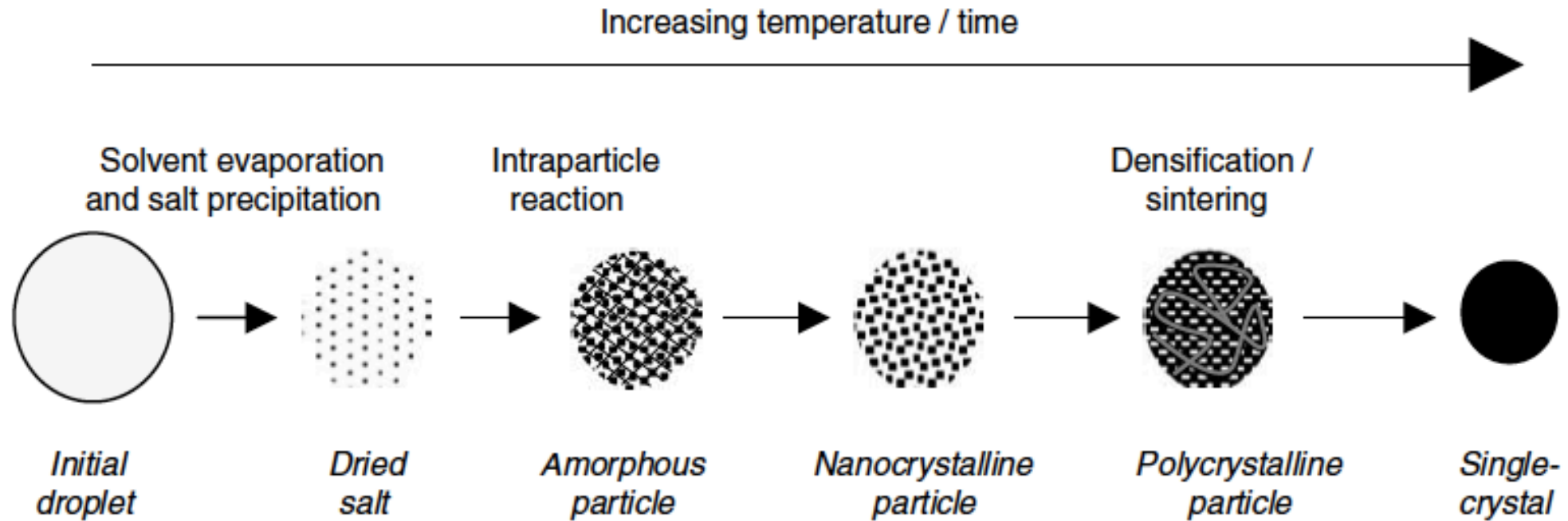
Nano-TiO₂ powders containing mixtures of anatase and rutile phases have been prepared by laser pyrolysis of TiCl₄ vapor, using air or nitrous oxide as oxygen carrier.

Ge NPs have been deposited on a Si substrate using an organogermanium precursor. By increasing the number of laser shots, the NPs could be converted to Si–Ge alloy structures.

Spray pyrolysis, which combines aspects of gas-phase processing and solution precipitation. The technique involves the formation of precursor aerosol droplets that are delivered by a carrier gas through a heating zone.

Precursor solutions of metal nitrates, metal chlorides, and metal acetates are atomized into fine droplets and sprayed into the thermal zone. Inside the heating zone, the solvent evaporates and reactions occur within each particle to form a product particle. Spherical, dense particles in the 100 to 1000 nm range can easily be formed in large volume by this method.

The principal advantage of the spray pyrolysis method is the ability to form multicomponent NPs as solutions of different metal salts can be mixed and aerosolized into the reaction zone.



Over the years, much emphasis has been given to being able to reduce the precursor droplet size during spray pyrolysis as this in turn would reduce the particle size.

Tsai et al. obtained uniformly sized dense and spherical particles of ~150 nm of yttria-stabilized zirconia by reducing the precursor concentration by about an order of magnitude.

In a modified version of the spray pyrolysis method, Che et al. synthesized SiO₂-encapsulated Pd NPs. These composite NPs were formed from a Pd-nitrate solution containing ultrafine SiO₂ particles by ultrasonic spray pyrolysis.

In spray pyrolysis, small droplets of a solution containing a desired precursor are injected into the hot zone of a furnace to obtain NPs.

The droplets are generated by using a nebulizer, generally by making use of a transducer. By controlling the nebulizer energy, the relative vapor pressures of the gases and the temperature of the furnace, the particle size is controlled.

Some examples of the use of spray pyrolysis are in the synthesis of Cu and TiO₂ NPs. Starting with different Cd precursors, CdS and CdSe NPs have been prepared.

A variant of this technique is flame spray pyrolysis, where the heat needed for the decomposition of the precursor is produced *in situ* by combustion. Mädler et al. applied this technique to synthesize SiO₂ NPs from hexamethyldisiloxane.

7. Laser Ablation

Laser ablation is mostly suited to metals, semiconductor, and ceramic NPs.

A pulsed excimer laser or a Nd:YAG laser is generally used.

Pulsed laser ablation (PLA) is a much faster and clean method to fabricate NPs directly from bulk targets than the chemical routes.

NPs can be directly produced by irradiating bulk targets, either in vacuum, in gas atmosphere, or in liquids with fast (nanosecond) and ultrafast (picosecond, femtosecond) laser pulses.

Table 1 Applications of lasers to materials processing

Technology
Cutting and hole drilling in metal slabs
Surface modification
Dry etching
Chemical vapor deposition
Pulsed laser deposition of semiconductor films
Pulsed laser ablation (PLA) deposition of metal films
PLA deposition of metal alloy films
PLA deposition of compound films
PLA deposition of high-critical-temperature superconductor films
Reactive PLA deposition of oxide, nitride, and carbide films

In the PLA, a powerful laser pulse vaporizes a target material placed in a vacuum chamber. Part of the vapor is collected on a substrate. PLA experienced an explosive growth since 1987, when it was used to deposit thin films of high-critical-temperature superconductors.

Laser ablation can be also performed in a low-pressure atmosphere to promote chemical reactions between the ablated material and the ambient atmosphere (reactive PLA, RPLA).

In 1985, laser vaporization of carbon targets led to the discovery of C60 and higher-mass fullerenes.

In the early stage of this technique, the main problem was the large size distribution of the produced NPs.

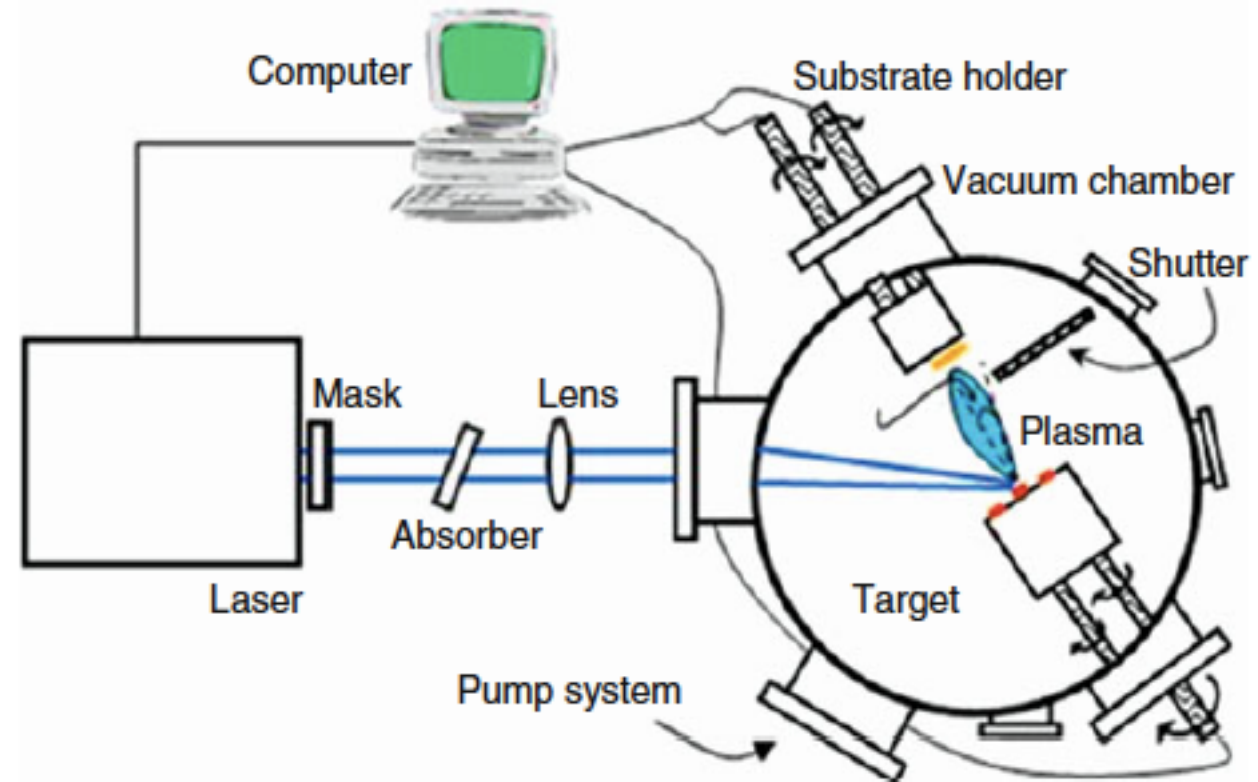
The accurate control and optimization of the ambient parameters like wavelength (λ), energy density (fluence, F), pulse duration (τ), pulse repetition rate (ν), and irradiation geometry is leading to an efficient tailoring of the NP size.

Advantage of the laser ablation method is that the target composition is faithfully reproduced in the NPs formed. For instance, nonstoichiometric $\text{VO}_{1.7}$ NPs obtained with target of a similar composition. The particles were subsequently oxidized to VO_2 .

Harfenist et al. prepared Ag NPs from this method and collected them in the form of a sol outside the preparation chamber.

Laser Ablation Mechanisms

Laser NP production is based on the ablation mechanism. The laser systems for NP production have the same components as the ones used for PLA deposition of thin films: a pulsed laser, a beam-handling optics, a target, and a substrate, usually placed in a vacuum chamber.



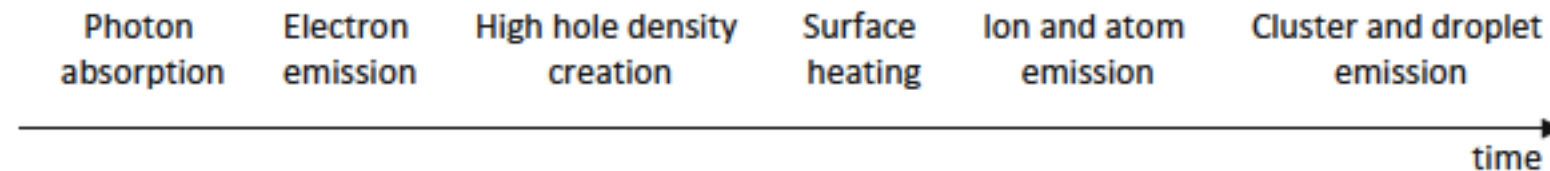
In laser excitations, the ionizing processes generate a number of free electrons, which in turn absorb laser photons. The free-electron gas transfers energy to the lattice by coupling to the vibrating ions, producing heating of the irradiated samples and triggering a whole range of phase-transformation processes, including melting and ablation via different mechanisms.

Table 2 Laser–material interaction mechanisms

Material	Interaction mechanism
Metals	Inverse bremsstrahlung
Semiconductors	Single-photon ionization
Low bandgap dielectrics	Single-photon ionization
Wide bandgap dielectrics	Multiphoton absorption ionization

Emission of electrons leaves behind positive holes. Time for bulk electrons to fill these holes is in picosecond (ps) or even longer. The surface-near region is positively charged for a considerable time. This charged region becomes electrostatically unstable at a sufficiently high hole density and the surface will break apart (Coulomb explosion) by emitting positive particles.

In semiconductors, strong levels of electronic excitation lead to bond breaking and lattice destabilization, producing ultrafast phase transitions. At very high excitation intensities, when hot carrier absorption becomes important, a hot electron bath is generated, rapidly coupling to the lattice via electron–phonon collisions, producing layer superheating, phase explosion, or explosive boiling. These processes are developed in pico- and nanosecond timescales, resulting in the ejection of a plasma plume, consisting of individual atoms/molecules, small clusters, and larger liquid droplets.



Many researchers modeled the PLA process under different environments (vacuum, buffer gas). A number of models describe the heating of the target on a macroscopic scale by considering the Fourier heat conduction equation with the laser energy as the source term. These models are accurate up to ns pulse duration. As the pulse duration decreases to picoseconds and femtoseconds (fs), the approach changes, considering microscopic interactions of the laser radiation with the target material.

The findings of the molecular dynamics (MD) simulations is the existence of well-defined threshold fluences for transitions from surface evaporation (desorption regime) to the collective material ejection (ablation regime). Particles/droplets and small atomic/molecular clusters are unavoidable products of the processes of material ejection in the ablation regime.

As early as in 1974, Kato produced NPs (“ultrafine particles,” since the term “nano” was not yet fashionable) by thermal evaporation of oxide targets (SiO_2 , MgO , Al_2O_3 , Fe_3O_4 , Mg_2SiO_4 , CaTiO_3 , and MgAl_2O_4) with a CO_2 laser beam (100 W) in inert gas (He, Ar, Xe). Kato found that most of the particles were spherical with a diameter of 10 nm, sticking to one another. Since the interest for NPs was far from starting, nobody was interested in this novel production mechanism.

Later, Gartner et al. used CO_2 laser to fabricate Y_2O_3 , SiO_2 , Al_2O_3 , and Cs_2O_3 NPs with mean size of 40 nm, depending on the gas (O_2 , Ar) pressure. NPs were produced by thermal evaporation of oxide targets, even if authors claim of “thermal ablation.”

Vijayalakshmi et al. produced Si NPs ($d = 4\text{--}5$ up to 25 nm) by PLA of $\langle 100 \rangle$ Si targets in vacuum ($\sim 10^{-3}$ Pa) with a KrF excimer laser ($\lambda = 248$ nm, $\tau = 8$ ns, $F = 191$ mJ/cm², $\nu = 50$ Hz). About 83 % of the NP crystallinity was seen to be from $\langle 111 \rangle$ and $\langle 220 \rangle$ Si. The authors observed that, since the NP crystallinity was different from that of the target, NPs should have formed in flight.

Kim et al. deposited Si NPs, but in He using an Nd:YAG laser ($\nu = 5$ Hz). The laser wavelength (355 , 532 , and $1,064$ nm), fluence ($1.0\text{--}2.5$ J/cm²), and ambient pressure (130 , 260 , 300 Pa) were varied to study the effect of growth conditions on the luminescent properties of Si NPs. The nanocrystallite size increased with increasing laser wavelength. Authors argued that, since penetration depth of radiation into Si increases with increasing wavelength, a deeper layer melts with consequent possibility of larger NP formation.

Complex oxide (CaFe_2O_4) pellets were ablated by Sasaki et al. with an ArF excimer laser ($\lambda = 193$ nm, $\tau = 17$ ns, $F = 0.4\text{--}1.6$ J/cm², $\nu = 10$ Hz). They controlled particle size and composition by varying the ambient gas pressure ($0.133\text{--}133$ Pa, $\text{O}_2 + \text{Ar}$ mixture). Increasing pressure increased particle size from 2 to 26 nm and reduced the Ca/Fe ratio from 0.9 to 0.2 .

Ogawa et al. produced titania, alumina, and iron oxide NP chain aggregates (NCA) by XeCl excimer laser ($\tau = 20$ ns) ablation of Ti, Al, and Fe targets in O_2 at a flow rate of $1\text{--}10$ l/min. Increasing laser frequency from 1 to 50 Hz at an oxygen flow rate of 1 l/min, the average NCA diameter increased from 79 to 132 nm.

Fang et al. studied ns-PLA of thin (5, 7.5 and 10 nm) Au films. After several hundreds of laser pulses of $2.5 \cdot 10^7$ W/cm² and $5 \cdot 10^7$ W/cm² intensity, uniformly distributed Au NPs with mean diameter of 10-25 nm were fabricated in an ultrafast melting, growing-up, and solidification process.

Recently, Au NPs layers were deposited at room temperature on poly (3,4-ethylene dioxythiophene)–poly(styrene sulfonate) (PEDOT:PSS) films by Resta et al. with the aim of fabricating efficient photovoltaic devices.

Bismuth NPs were deposited on dielectric (Al₂O₃) thin films in vacuum ($\sim 10^{-7}$ Pa) by Garcia-Velenzuela et al. using an ArF excimer laser ($\tau = 12$ ns, $\nu = 2$ Hz). Well-separated NPs with a quasi-circular shape and $d = 10$ nm were observed after 50 laser pulses. After 100 pulses, coalescence led to the formation of bigger NPs with size distribution up to ~ 100 nm.

The effect of a radiofrequency (rf) field (150 W) during PLA of W targets with 12,000 Nd:YAG laser pulses ($\lambda = 355$ nm, $\tau = 5$ ns, $F = 4.5$ J/cm², $\nu = 10$ Hz) either in pure O₂ or in an O₂ + He mixture, at a total pressure of 700 and 900 Pa. The authors observed that the reactivity in gas phase is increased by excited/ionized oxygen molecules and atoms produced by the rf discharge.

By changing the pulse duration from nanoseconds (ns) to picoseconds (ps) toward femtoseconds (fs), the ablation mechanism changes.

Shorter pulse durations result in higher peak power densities and larger electric fields at comparable fluences.

Another advantage of ultrashort pulses is the decreased thermal diffusion into the target during the laser pulse.

So, subsurface boiling, resulting in ejection of micron-sized particles, is minimized.

Moreover, the latter part of ns pulses is partially absorbed by the emerging plasma plume, while ps pulses interact to a lesser extent and fs pulses do not interact at all.

An unexpected finding was the influence of the laser beam spot size.

In the case of the smaller beam spot size, the emission of micron-sized droplets was evidenced, while for larger beam spot sizes, solely NP emission was observed.

Laser Fabrication of Nanoparticles in Liquids

The equipment for PLA in liquids is simpler, since vacuum chambers are not required. It consists of a pulsed laser, a set of focusing optics, and a vessel containing a liquid and the target material. The process is commonly called LAL (Laser Ablation in Liquids).

A major advantage of LAL is that NPs can be obtained in water or organic solvents (Toluene, DMSO, DMF, THF, AcCN, acetone) without chemical precursors, stabilizing molecules, or ligands.

The main formation mechanism consists in nucleation during the plasma plume cooling followed by growth and coalescence.

Low fluences are associated with NPs with small average diameters (3-6 nm) and ascribed to the vaporization of the target.

High fluences are associated with larger NPs, having a size distribution peaked at tens of nanometers, and ascribed to the explosive boiling of the target.

However, NPs can have different sizes, since the atomic density and the temperature profiles are not homogeneous in the plasma plume.

LAL was pioneered by Fojtik and Henglein in 1993. They used a ruby laser ($\lambda = 694 \text{ nm}$) to ablate films of gold, nickel, and carbon in water, 2-propanol, and cyclohexane. Colloidal solutions of these materials were obtained.

Gold, silver, and platinum NPs have been produced by LAL using different lasers and with variable results in terms of average size and size distribution.

The type of material, solvent, and laser parameters like wavelength, time duration, and fluence has effective parameters.

De Bonis et al. performed PLA of a titanium target in water by a Ti: sapphire source ($\lambda = 800 \text{ nm}$, $\tau = 100 \text{ fs}$, $\nu = 1 \text{ kHz}$). Analyses revealed the presence of TiO_x NPs with a certain amount of crystalline rutile phase. Upon aging in water, the formation of a lamellar phase was observed, which rolled up to microtubes by remaining in water for one month, through a self-assembling process.

The formed microtubes, with an inner diameter of about $2 \mu\text{m}$ and an outer diameter of $4 \mu\text{m}$, are characterized by a smooth interior surface and aggregation of NPs on the outer surface.

An organic NP synthesis was demonstrated by Elaboudi et al. by underwater KrF excimer laser ($\tau = 25$ ns) ablation of polycarbonate. The polycarbonate film was partly ablated into NPs with size ranging from 8 to 180 nm, by adjusting the number of ablating pulses.

By irradiation of organic microcrystals suspended in water, Asahi and coworkers observed photothermal or photomechanical ablation mechanisms with ns and fs laser pulses, respectively.

Narayan et al. synthesized Pd NPs starting from a solution of $\text{PdCl}_2 + \text{NH}_3 + \text{H}_2\text{O}$ by photolytic decomposition of their amine complexes using an ArF laser (193 nm, 15 ns, $F = 120$ mJ/cm², up to 60 Hz).

PLA was demonstrated to be an efficient and clean method to fabricate metal, oxide, semiconductor, and even organic NPs. Using PLA in vacuum, NPs can condense at the substrate surface (low laser fluences) and their dimensions can be roughly controlled by the pulse number or be directly emitted by the target (high fluences). Gas atmosphere can help in controlling NP size, via enhanced collisions in the denser plasma plume.

However, PLA fabrication of NPs still has some important drawbacks, mainly the accurate control on the NP average size and size distribution.

Duration of laser pulses is an important parameter.

Femtosecond laser pulses release energy to electrons in the target on a timescale much faster than electron–phonon thermalization processes, while picosecond and nanosecond laser pulses release energy on a timescale comparable with the thermal relaxation processes of the target.

Laser intensity is a fundamental parameter, which determines evaporation or explosive boiling of the target surface layer.

Wavelength determines penetration into the target material. At the same fluence, a thicker layer could be ablated using longer wavelength, producing bigger NPs.

One of the main advantages of LAL is the ability to obtain ligand-free NPs in a variety of solvents. Functionalization with desired molecules can be obtained by choosing the solvent suitable for particle synthesis and molecule solubilization.

The solvent can influence NP dimensions: diameters of ~10-40 nm are typical of NPs obtained in water, while smaller sizes (~5-15 nm) were observed in organic solvents, due to the different thermal properties of water with organic solvents or to a strong interaction of organic solvents with the surface of NPs, which is competitive with particle growth.

Among the peculiarities which are determining the success of LAL technique, it must be mentioned the fact that the experimental setup is quite simple and the process is fast and can be used as a unitary approach for the synthesis of different materials, in different solvents, with different surface functionalizations.

It is a “green” technique with respect to any other chemical route.

SOLUTION PROCESSING OF NANOPARTICLES

Precipitating clusters of inorganic compounds from a solution of chemical compounds has been an attractive primarily because of the simplicity with which experiments can be conducted in a laboratory. This is especially true if the goal is to just have a nanocrystalline powder, instead of a “dispersible” nanoparticulate powder.

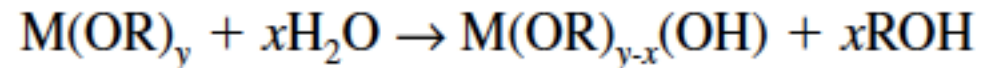
A major advantage of solution processing is the ability to form encapsulated NPs, specifically with an organic molecule, for providing functionality to the NPs, improving their stability in a medium, or for controlling their shape and size.

1. SOL-GEL PROCESSING

Sol-gel technique is one of the most popular solutions processing method for producing metal oxide NPs. Over the years, solution precipitation and sol-gel processing have come to be used interchangeably.

In sol-gel processing, a reactive metal precursor, such as metal alkoxide, is hydrolyzed with water, and the hydrolyzed species are allowed to condense with each other to form precipitates of metal oxide NPs. The precipitate is subsequently washed and dried, which is then calcined at an elevated temperature to form crystalline metal oxide NPs.

The hydrolysis of metal alkoxides involves nucleophilic reaction with water, which is as follows:



Condensation occurs when either hydrolyzed species react with each other and release a water molecule, or a hydrolyzed species reacts with an unhydrolyzed species and releases an alcohol molecule.

The rates at which hydrolysis and condensation reactions take place are important parameters that affect the properties of the final product. For example, slower and more controlled hydrolysis typically leads to smaller particles, and base-catalyzed condensation reactions form denser particles.

2. SOLUTION PRECIPITATION

In the precipitation method, an inorganic metal salt (e.g., chloride, nitrate, acetate, or oxychloride) is dissolved in water. Metal cations in water exist in the form of metal hydrate species, such as $\text{Al}(\text{H}_2\text{O})^{3+}$ and $\text{Fe}(\text{H}_2\text{O})_6^{3+}$.

These species are hydrolyzed by adding a base solution, such as NaOH or NH_4OH . The hydrolyzed species condense with each other to form either a metal hydroxide or hydrous metal oxide precipitate on increasing the concentration of OH ions in the solution.

The precipitate is then washed, filtered, and dried. The dried powder is subsequently calcined to obtain the final crystalline metal oxide phase.

The major advantage of this process is that it is relatively economical and is used to synthesize a wide range of single- and multi-components oxide nanopowders.

Additionally, nanocomposites of metal oxides are also produced by co-precipitation of corresponding metal hydroxides.

One of the major drawbacks of the process as described above is the inability to control the size of particles and their subsequent aggregation.

Significant efforts have been made to control particle characteristics, such as surface area and aggregate size, by precipitating in the presence of a surfactant or an organic molecule.

Hudson and Knowles synthesized mesoporous, high surface area zirconium oxide by incorporating cationic quaternary ammonium surfactants in the hydrous oxide and subsequent calcination of the inorganic/organic intermediate.

The pore size distribution and surface area of zirconium oxide nanopowders were modified by changing the length of the hydrophobic chain from C₈ to C₁₈.

Fokema et al. demonstrated that changing the precipitating agent from ammonium hydroxide to tetraalkylammonium hydroxide results in a decrease in the primary particle size of yttrium oxide.

The reason was attributed to the higher pH of tetraalkylammonium hydroxide in comparison to ammonium hydroxide, and the steric effect of tetraalkylammonium cation to reduce the diffusion of soluble precursors to the particle surface.

A hydrodynamic cavitation process is introduced by combining the aspects of different solution precipitation techniques.

Nanocrystalline oxide ceramic particles in the range nm to micron have been produced by hydrodynamic processing in a microfluidizer.

The method of producing oxide NPs involve a co-precipitation of the metal oxide components.

The precipitated gel experiences ultrashear forces and cavitation heating. These two aspects lead to the formation of nanophase particles and high-phase purity in complex metal oxides.

3. Micelles and Microemulsions

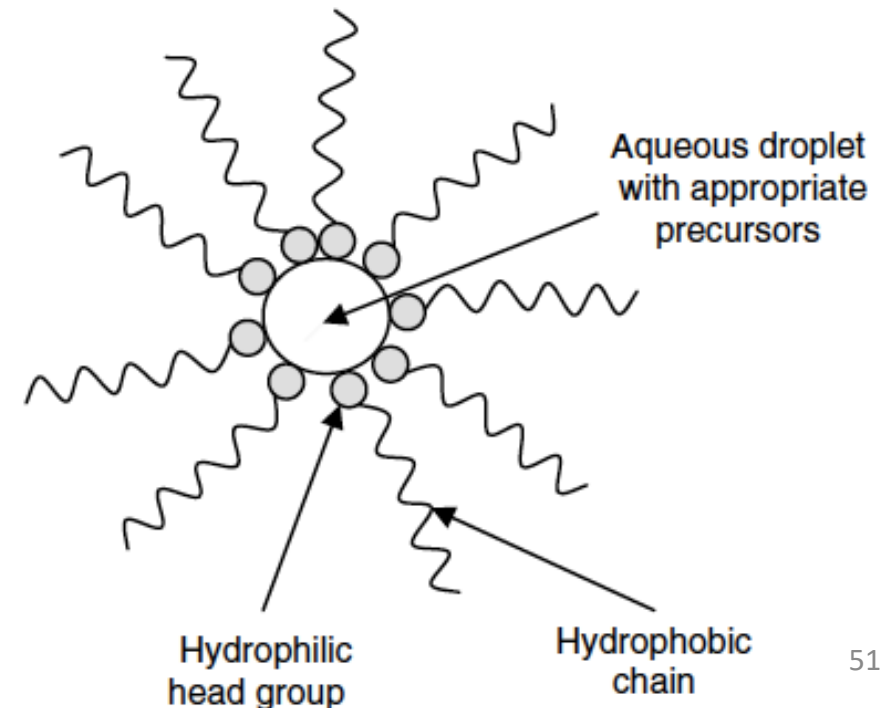
Uniform and size-controlled NPs of metal, semiconductor, and metal oxides can be produced by the water-in-oil (W/O) microemulsion (also called reverse micelle) method.

In a W/O microemulsion, nanosized water droplets, stabilized by a surfactant, are dispersed in an oil phase. A micelle is designated inverse or reverse when the hydrophilic end of the surfactant points inward rather than outward as in a normal micelle.

Nanosized water droplets act as a microreactor, wherein particle formation occurs and helps to control the size of NPs.

A unique feature of the reverse micelle process is that the particles are generally nanosized and monodisperse.

This is because the surfactant molecules that stabilized the water droplets also adsorb on the surface of the NPs, once the particle size approaches that of the water droplet.



The dimensions of the water droplet can be suitably altered by changing the concentration of the surfactant and water.

In reverse micelle technique, water droplets (carrying appropriate reactants) are allowed to collide with each other and the particle forms inside the water droplet.

NP synthesis is accomplished by one of the two different chemical reactions:

- (i) hydrolysis of metal alkoxides or precipitation of metal salts with a base, in case of metal oxide NPs, and
- (ii) (ii) reduction of metal salts with a reducing agent, such as NaBH_4 , in case of metal NPs.

Precipitation of the micelle with a polar solvent helps to recover the NPs.

Particles are either filtered or centrifuged and then washed with acetone and water to remove any residual oil and surfactant molecules adsorbed on the surface NPs.

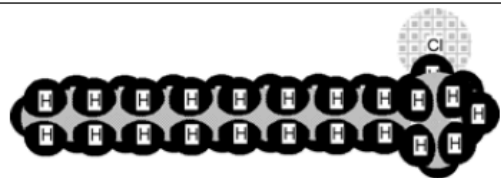
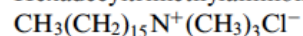
Recent advances have tended to focus on methods for efficient recovery of NPs. A method to overcome the particle separation is using water-in-supercritical CO_2 micro-emulsion, since CO_2 can be easily removed by decreasing the pressure.

Subsequently, the powders are calcined to form the final product.

TABLE I.1. Structure of some typical surfactant molecules

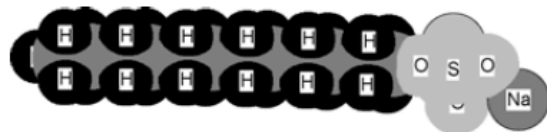
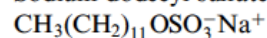
1. Cationic surfactants

Hexadecyltrimethylammonium chloride, CTAC

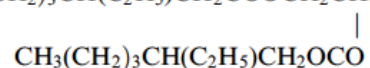
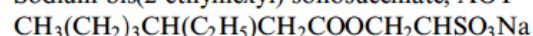


2. Anionic surfactants

Sodium dodecyl sulfate, SDS

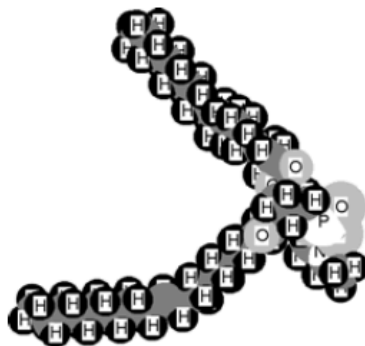
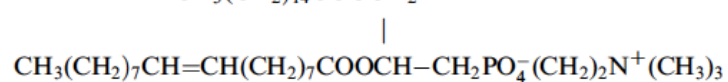
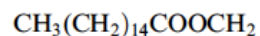


Sodium bis(2-ethylhexyl) solfosuccinate, AOT



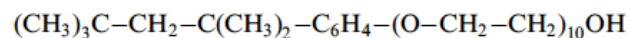
3. Zwitterionic surfactants

Lecithin



4. Nonionic surfactants

Triton X-100



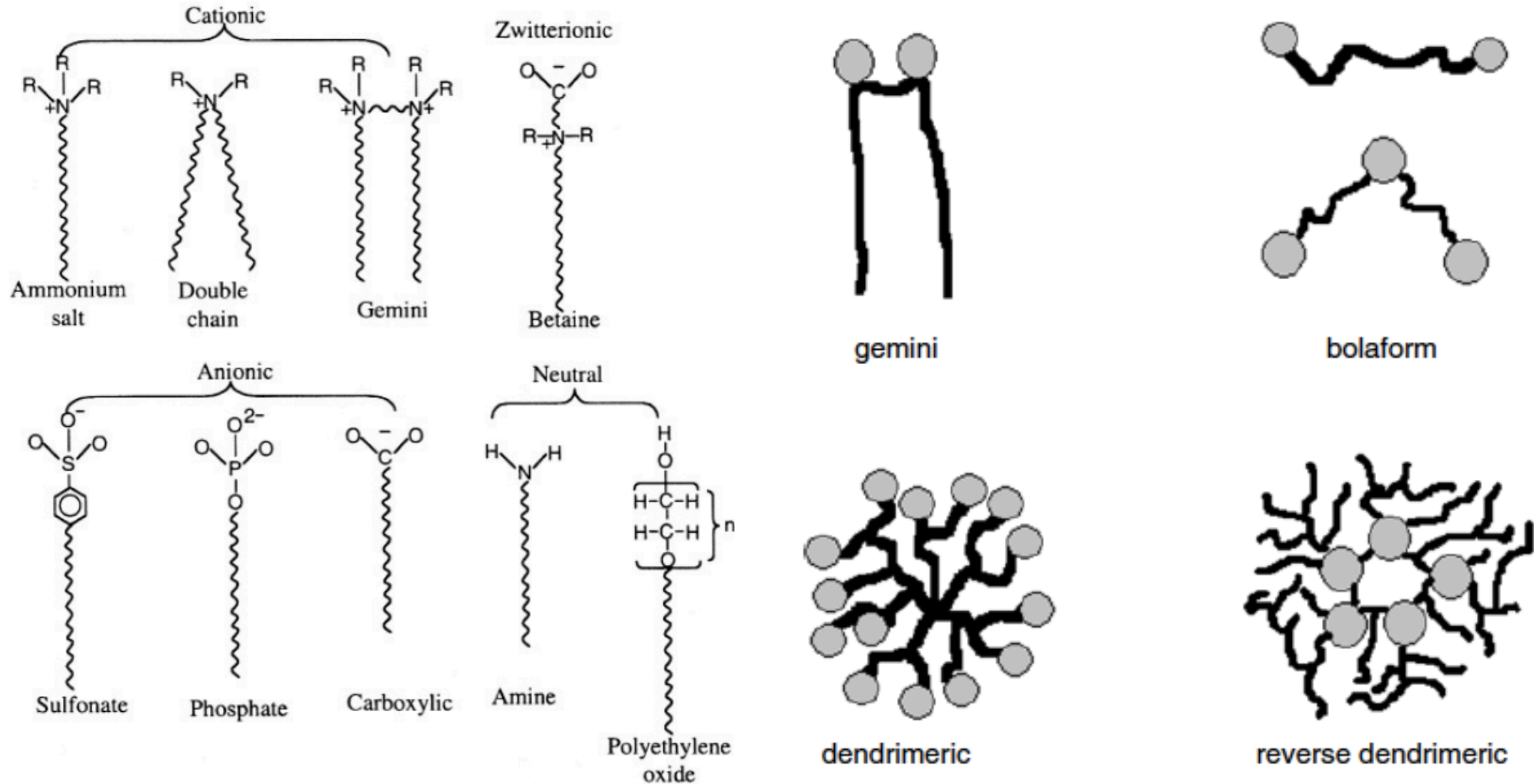
Surfactant molecules are characterized by molecular anisometry, i.e. elongated shape, wide spectrum of molecular conformations, and the coexistence of spatially separated hydrophobic (only polarizable) and hydrophilic (both polar/ionic and polarizable) moieties.

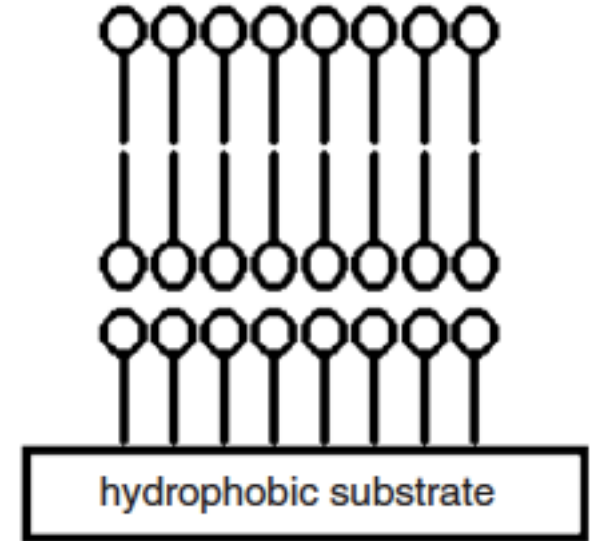
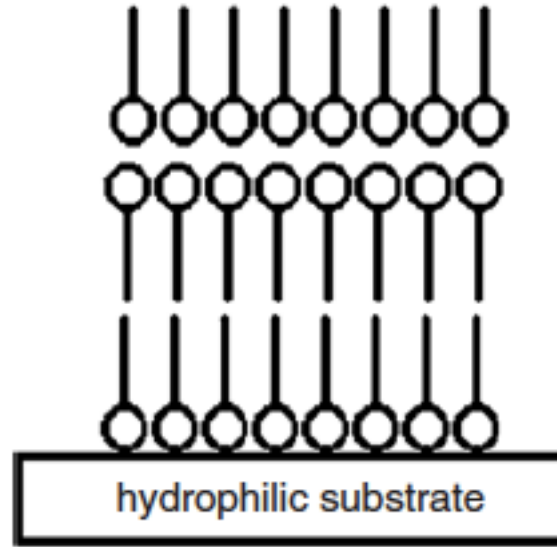
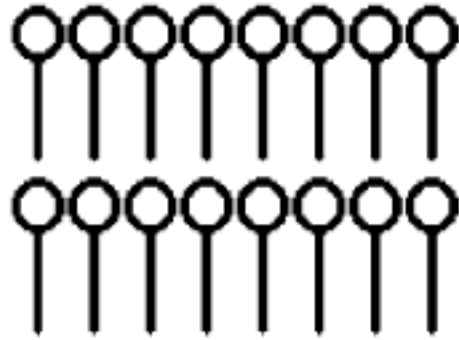
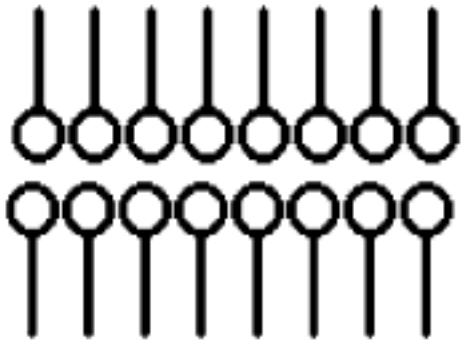
The hydrophobic part is constituted by one or more long and flexible hydrocarbon or fluorocarbon chains, whereas the hydrophilic one is generally concentrated in a smaller domain of the entire molecule and is formed by a polar or ionic head group.

Depending on the nature of the head group attached to the alkyl chains, surfactants are distinguished as non-ionic (polar), ionic (cationic or anionic), and zwitterionic (carrying both positive and negative charged groups).

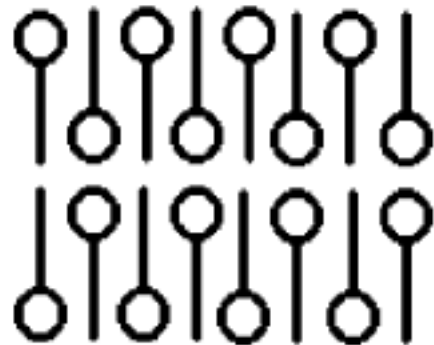
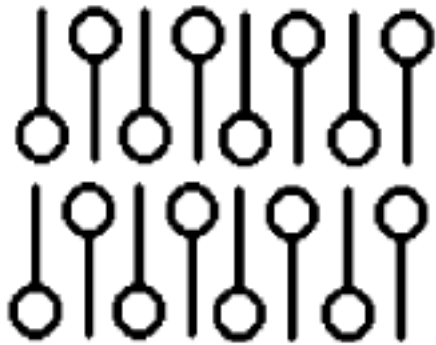
In the case of anionic surfactants, the presence of some metal ions as counterions could provide additional features such as color, magnetism, and catalytic capability.

Recent developments in the synthesis of surfactants have led to novel classes such as polymerizable, polymeric, Gemini, glycolipidic, dendritic, bolaform, and multifunctional surfactants, or according to their potential applications as hydrophilic, lipophilic, photosensitive, degradable, biocompatible, and eco-compatible surfactants.



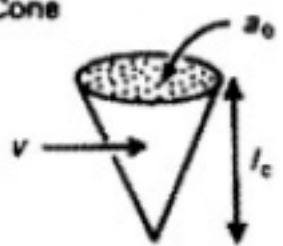
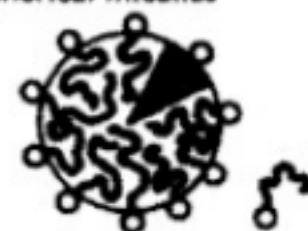

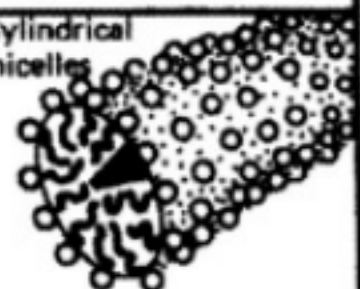

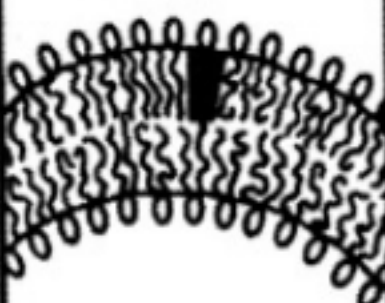


Self-assembled multilayers of surfactant molecules on hydrophilic or hydrophobic substrates

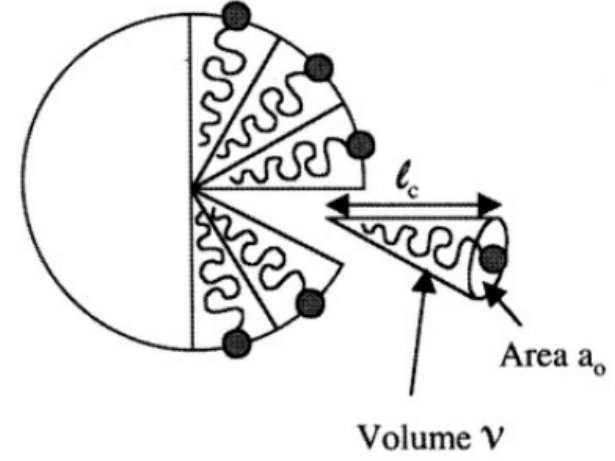


Arrangements of surfactant molecules in the plane


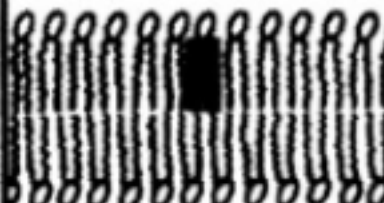

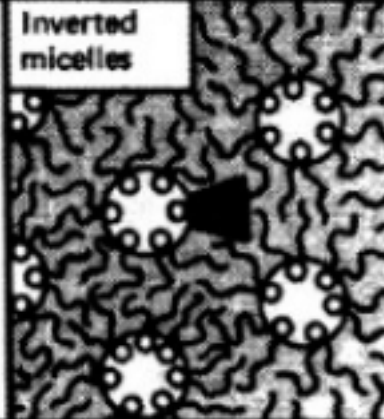


Critical packing parameter v/a_0l_c	Critical packing shape	Structures formed
$< 1/3$	Cone 	Spherical micelles 
$1/3-1/2$	Truncated cone 	Cylindrical micelles 
$1/2-1$	Truncated cone 	Flexible bilayers, vesicles 

Surfactants not only influence the size and shape of the NPs, but also arrange them into highly organized nanostructures.



Critical packing parameter
 $R = v/a_0l_c$

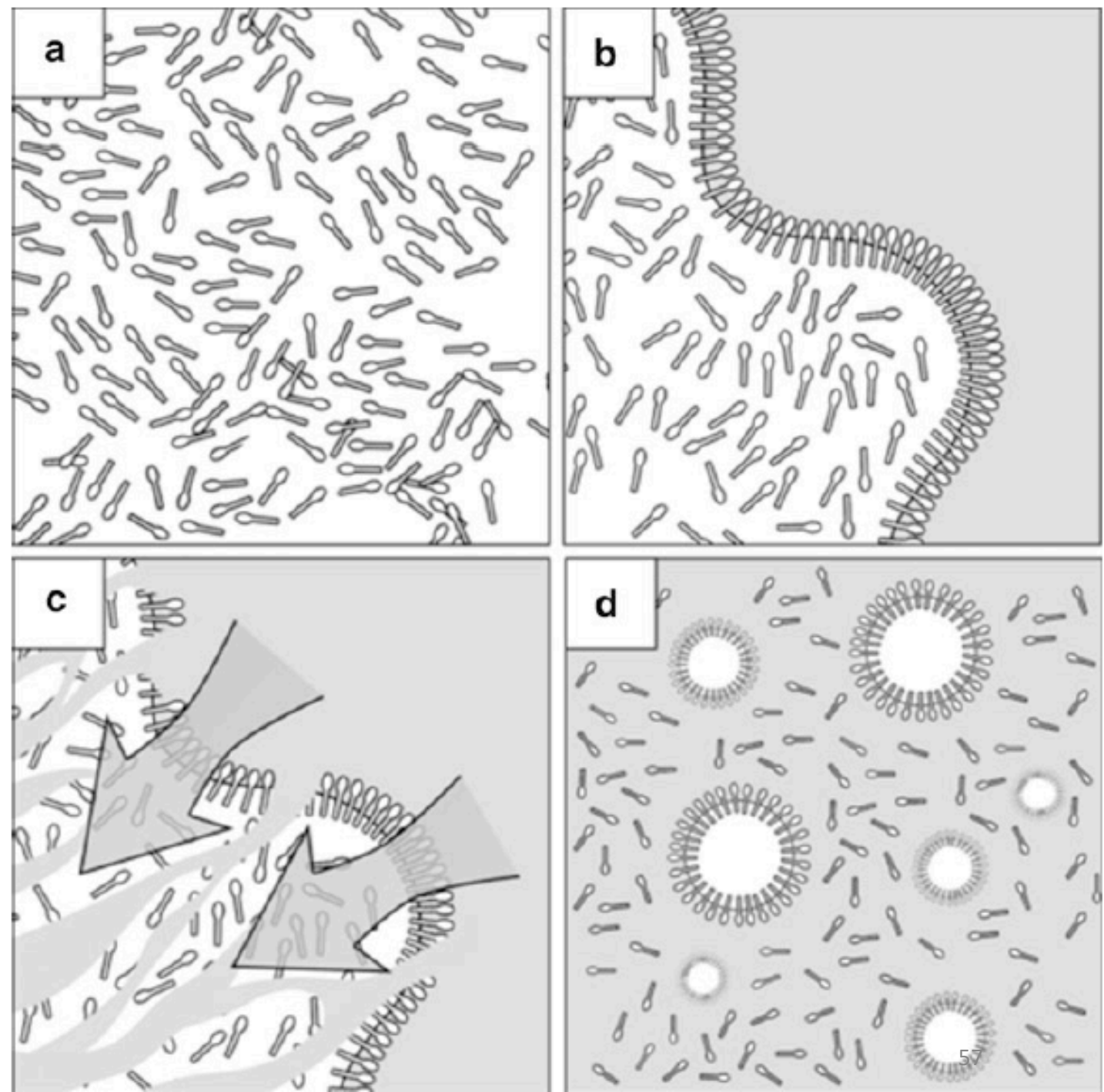
~ 1	Cylinder 	Planar bilayers 
> 1	Inverted truncated cone or wedge 	Inverted micelles 

a: Homogeneous mixing of surfactant in oil (i.e., solubilized or dispersed).

b: The surfactant/oil phase is mixed with the aqueous phase (e.g., pure water).

c: The water phase penetrates the former very rapidly in order to solubilize the surfactant molecules.

d: Small nanometric oily drops with a very narrow size distribution are immediately generated and stabilized with surfactants.



Nano-emulsion systems consist of a suspension of liquid nanodroplets stabilized by surfactants.

Emulsions are thermodynamically unstable systems because the free energy ΔG_f is greater than zero. Considering the global expression $\Delta G_f = \gamma \Delta A - T \Delta S_f$ (with γ the water-oil interfacial tension, ΔA the water-oil interfacial area gained with emulsification, $T \Delta S_f$ the entropy of droplet formation). The emulsion instability only comes from ΔA , and ΔG_f can be reduced with playing on the interfacial tension γ .

The physical destabilization of emulsions is related to the spontaneous trend towards a minimal interfacial area between the two immiscible phases. Minimization of interfacial area is attained by two mechanisms: (i) flocculation followed mostly by coalescence and (ii) Ostwald ripening.

Nano-emulsions are thermodynamically unstable systems, but kinetically stable, and stable against fluctuations of thermodynamic variables like temperature fluctuations or dilution.

Nano-emulsion flocculation is naturally prevented by steric stabilization. When interfacial layers of two different droplet layers overlap, steric repulsion arises.

Emulsion under pressure

At low surfactant concentration, $C < (\text{critical micelle concentration})/10$, the applied pressure does not influence the size of the homogenized droplets.

During processing, drops are efficiently fragmented, they undergo a strong coalescence owing to the inefficient surface stabilization by surfactant due to their low concentration.

As a result, the droplet size cannot be decreased below 300 nm.

At high surfactant concentration, for $C > (\text{critical micelle concentration}) * 10$, the newly fragmented droplets are largely stabilized by surfactant before coalescence, allowing decreasing the size up to 50 nm.

This is due to the surfactant interfacial adsorption time being shorter than the recombination and coalescence time.

The first reported synthesis of NPs using microemulsions was by Boutonnet et al. who synthesized Pt, Pd, Rh, and Ir NPs by reducing the corresponding metal salts with hydrogen or hydrazine in microemulsions.

Pileni et al. synthesized CdS nanocrystals by using the *iso*-octane-sodium bis(2-ethylhexyl)sulfosuccinate (commonly called AOT or Aerosol-OT)-water system. The *iso*-octane/water system has been used to prepare NPs of Cu, Ag, Ag₂S, AgI, etc.

The relation between the relative concentrations of the surfactant (AOT) and water ($\omega = [\text{H}_2\text{O}]/[\text{AOT}]$) and the water pool radius (R, in nanometers) has been worked out.

For values of ω upto 15, the following relation holds: $R = 0.15\omega$ (2.4)

Zhang et al. have synthesized MnFe₂O₄ particles using an inverted micelle template. The control over the size of the nanocrystals is achieved by altering ω . The dependence is often nonlinear, probably because the structure of water in the pool is different from that in the bulk.

Surfactants form inverted micelles in oil medium without the use of water. Dry powders of salts can be dispersed in the surfactant solution and reduced with reducing agents such as LiBH₄ and Na in oil.

Wilcoxon et al. have made use of this method to synthesize Au, Si, and Ge nanocrystals. Si and Ge nanocrystals were obtained by dispersion of the halides in an inverted micelle followed by reduction with LiAlH₄ in THF.

Pileni et al. have pioneered the use of oil in water (O/W) micelles to prepare particles of CoFe_2O_4 , $\gamma\text{-Fe}_2\text{O}_3$, and Fe_3O_4 .

The basic reaction involving hydrolysis is templated by a micellar droplet. The reactants are introduced in the form of a salt of a surfactant such as sodium dodecyl sulphate (SDS). Thus, by adding $\text{CH}_3\text{NH}_3\text{OH}$ to a micelle made of calculated quantities of $\text{Fe}(\text{SDS})_2$ and $\text{Co}(\text{SDS})_2$, NPs of CoFe_2O_4 are obtained.

By increasing the concentration of metal salts, the size of the NPs can be increased. This method has been extended for the synthesis of Cu NPs.

Sastry et al. have made use of aqueous foams as templates to form platelets and particles of Au. A foam is generated in a column by the use of the surfactant CTAB (cetyltrimethylammonium bromide) complexed with HAuCl_4 .

The Au ions dispersed over the foam are reduced by a gaseous reductant such as hydrazine vapors. It is supposed that the platelets are produced by reduction of the CTAB–Au complex molecules at the bubble walls, while the same complex molecules at the interbubble voids provide the isotropic space required for the generation of spherical particles.

Microemulsions made of water in supercritical fluids such as CO_2 have been used to synthesize NPs of Ag, Ir, and Pt.

4. Solvothermal synthesis

The solvothermal method provides a means of using solvents at temperatures above their boiling points, by carrying out the reaction in a sealed vessel. The pressure generated in the vessel due to the solvent vapors elevates the boiling point of the solvent.

Solvents such as ethanol, toluene, and water, and are widely used to synthesize zeolites, inorganic open-framework structures, and other solid materials.

In the past few years, solvothermal synthesis has emerged to become the chosen method to synthesize nanocrystals of inorganic materials. Numerous solvothermal schemes have been employed to produce nanocrystalline powders as well as nanocrystals dispersible in a liquid.

Qian et al. have reported several solvothermal routes to chalcogenide nanocrystals. CdS nanocrystals of 6 nm diameter have been made using cadmium sulphate/nitrate as the Cd source, thiourea as the S source and ethylene glycol as the solvent. The reaction was carried out for 12 h at 180 °C.

Chen and Fan have prepared transition metal dichalcogenides (MS_2 ; M = Fe, Co, Ni, Mo; S = S or Se) with diameters in the range 4–200 nm by a hydrothermal route (water as solvent).

Fe, Co, and Ni chalcogenides were obtained by treating the corresponding halide with $\text{Na}_2\text{S}_2\text{O}_3$ (sodium thiosulphate) or $\text{Na}_2\text{Se}_5\text{O}_3$ (sodium selenosulphate) for 12 h at 140–150 °C. Mo chalcogenides were prepared starting from Na_2MoO_4 , sodium thio or seleno sulphate and hydrazine.

By employing a metal salt, elemental Se or S and a reducing agent (to reduce Se or S), it is possible to produce metal chalcogenide nanocrystals. Control over size is rendered possible by the slow release of sulphide or selenide ions. Nanocrystal dispersions are often obtained even without a capping agent.

CdSe nanocrystals have been prepared solvothermally by reacting Cd stearate with elemental Se in toluene in the presence of tetralin. CdS nanocrystals are similarly prepared by the reaction of a Cd salt with S in the presence of tetralin.

Wei et al. report a green synthetic route for CdSe NPs in aqueous solution using Se powder as the selenium source. CdS nanocrystals of ~6 nm diameter have also been prepared in an aqueous solution at room temperature.

A low-temperature one-pot synthesis of HgTe nanocrystals has been described without the use of toxic precursors.

Nanocrystals of chalcogenides can be prepared under solvothermal conditions starting with the elements. ZnSe nanocrystals of 12–16 nm are prepared by reacting the elements in pyridine. By reacting Zn and Se in ethylenediamine, a complex ZnSe(en) is obtained. This compound gets thermally decomposed to yield ZnSe NPs.

Peng et al. have obtained ZnSe and CdSe NPs in the 70–100 nm size range by combining the elements under hydrothermal conditions. ZnS NPs in the 3–18 nm size range have been obtained by Qian et al. by treating Zn and S in pyridine.

A surfactant-assisted solvothermal procedure has been employed to prepare PbS nanocrystals at 85 °C.

A solvothermal reaction in the presence of octadecylamine yields monodisperse PbSe nanocrystals of controllable size.

Large GaN nanocrystals (32 nm) have been produced by Xie et al. by treating GaCl₃ with Li₃N in benzene. Sardar and Rao have prepared GaN NPs of various sizes under solvothermal conditions, employing gallium cupferronate (Ga(C₆H₅N₂O₂)₃) or chloride (GaCl₃) as the gallium source and hexamethyldisilyzane as the nitriding agent and toluene as solvent.

By employing surfactants such as CTAB, the size of the nanocrystals could be controlled.

This method has been applied for the synthesis of AlN, GaN, and InN nanocrystals. The procedure yields nanocrystals with an average diameter of 10 nm for AlN, 15 nm for InN, and 4 nm for GaN.

InP NPs of different sizes (12–40 nm) have been prepared by the solvothermal reaction involving InCl_3 and Na_3P . The size of the particles could be varied by changing the solvent from coordinating dimethoxyethane to noncoordinating benzene.

The reaction of metal acetylacetonates under solvothermal conditions produces nanocrystals of metal oxides such as Ga_2O_3 , ZnO, and cubic In_2O_3 .

CoO NPs with diameters in 4.5–18 nm range have been prepared by the decomposition of cobalt cupferronate in decalin at 270 °C under solvothermal conditions.

Cubic and hexagonal CoO nanocrystals have also been obtained starting from $\text{Co}(\text{acac})_3$.

5. Sonochemical synthesis

The effect of ultrasound on a colloidal system has been known for preparation of nanomaterials.

In order to carry out sonochemical reactions (ultrasound-assisted method), a mix of reagents dissolved in a solvent is subjected to ultrasound radiation (20 kHz–10 MHz).

The basic idea of sonochemistry arises from acoustic cavitation, which leads to the creation, growth, and collapse of bubbles in the liquid medium that results high pressure as well as temperature followed by high cooling rate.

The creation of bubbles is due to the suspended particulate matter and impurities in the solvent.

The growth of a bubble by expansion leads to the creation of a vacuum that induces the diffusion of volatile reagents into the bubble. The growth step is followed by the collapse of the bubble which takes places rapidly accompanied by a temperature change of 5,000–25,000 K in about a nanosecond.

Collapse of the bubble triggers the decomposition of the matter within the bubble. The rapid cooling rate often hinders crystallization, and amorphous products are usually obtained.

In the process of cavitation, generated bubble collapse producing intense heat with high pressures (1,000 bar) in short time period, which drives high-energy chemical reactions.

The collapse is frequently accompanied by the formation of free radicals that cause further reactions. A few of the sonochemical reactions are mediated by free radicals.

In detail, acoustic waves (alternating expansive and compressive) by ultrasonic irradiation of liquid produce bubbles (cavities) and make them oscillate. These bubbles store ultrasonic energy very efficiently during their growth. A bubble can overgrow and subsequently collapse, releasing stored ultrasonic energy within short time period (heating and cooling rate of $>10^{10} \text{ K s}^{-1}$).

Different types of sonochemical apparatus are used for the production of ultrasonic waves like ultrasonic horns, ultrasonic cleaning baths, and flow reactors.

For most of the applications, intensity of ultrasonic baths is inadequate, but is however suitable for liquid–solid reactions.

In typical laboratory-scale reactions, high intensity ultrasonic titanium horn with piezoelectric transducer is preferred. The process of cavitation occurs over a wide array of frequencies (10 Hz–10 MHz).

The concept of sonochemistry is associated to a low frequency with high-intensity ultrasound (typically 20 kHz), whereas ultrasonic spray pyrolysis (USP) usually utilize a high frequency with low-intensity ultrasound (e.g., 2 MHz).

In accordance with traditional techniques, USP has several advantages like continuous operation technique, easy control, and high product purity.

Baigent and Muller reported sonochemical method to synthesize colloidal Au by reduction of HAuCl_4 in an aqueous medium. By the use of PVP, the stability of the colloids is improved. The introduction of alcohols in the reducing mixture, enhances the rate of formation of the Au particles. At high alcohol concentrations, smaller NPs are formed.

A mechanism based on the ability of alcohols to scavenge the H and the OH radicals has been proposed. Increasing the hydrophobicity of alcohols reduces the size of the NPs due to the increasing ability of the hydrophobic alcohols to cap the produced NPs.

This method has been extended to prepare Pt NPs, starting from chloroplatinic acid solutions containing ethyl alcohol. Maeda et al. used sodium dodecyl sulphate (SDS) as the stabilizing agent to obtain Pt NPs of 2.6 nm diameter. The sonochemical reduction of Pd and Pt salts starting from K_2PdCl_4 and H_2PtCl_6 have been carried out under inert atmospheres.

Pd NPs in the size range 5–100 nm are obtained from aqueous solutions of PdCl₂ in the presence of stabilizing agents such as SDS, PVP, and poly(oxyethylene sorbitan monolaurate).

Maeda et al. have obtained Ag nanocrystals by the sonochemical reduction of aqueous AgClO₄ and AgNO₃ in the presence of SDS. The average size of the particles obtained by the above methods are between 10 and 20 nm.

Gedanken et al. have prepared 20 nm sized Ag NPs by the sonochemical reduction of AgNO₃ without the aid of capping agents.

Metallic Cu NPs have been obtained by the ultrasonic irradiation of copper hydrazine carboxylate in water. The reaction is believed to be mediated by hydrogen radicals.

Sonochemical treatment of volatile organometallic precursors dissolved in less-volatile solvents helps in the selective decomposition of the precursors. This method was first used by Suslick et al. to prepare colloidal Fe, by the decomposition of Fe(CO)₅ in octanol. With PVP as the capping agent, the particle diameters obtained were in the 2–8 nm range, while oleic acid yielded monodispersed NPs with an average diameter of 8 nm.

Gadenken et al. extended this method to prepare Co, Ni and Fe₂O₃ NPs. Co NPs stabilized by oleic acid were obtained in decalin, while oleic acid capped Fe₂O₃ NPs were obtained in hexadecane. Ni particles could be prepared starting with Ni(CO)₄ in decane.

Organosols of Pd have also been obtained by the sonochemical reduction of $\text{Pd}(\text{O}_2\text{CCH}_3)_2$ and myristyltrimethylammonium bromide in THF or methanol.

Luminescent Si NPs obtained by the sonochemical reduction of TEOS with a colloidal solution of Na in toluene. Si nanocrystals have been prepared by ultrasonically dispersing porous Si.

Grieser et al. obtained CdS NPs by sonochemical means, starting with mixtures of Cd salts, water soluble thiols such as 2-mercaptopropanoic acid and sodium polyphosphate. The sulphide ions were generated by the reaction of thiols with hydrogen radicals. CuS and PbS NPs have also been prepared.

By the ultrasonic irradiation of a mixture of metal salts and selenium in ethylene diamine, Li et al. have obtained Ag, Cu, and Pb selenides.

A sonochemical method for the synthesis of hollow MoS_2 nanocrystals has been described.

$\text{BaFe}_{12}\text{O}_{19}$ NPs could be prepared by high-intensity sonication of a solution containing $\text{Fe}(\text{CO})_5$ and barium ethylhexonate in decane, followed by calcination of the resulting powder at 900 K. After calcination, the particles were dispersible without the use of surfactants.

InP NPs have been prepared by the ultrasonic irradiation of InCl_3 , KBH_4 , and yellow P in benzene and ethanol.

6. Microwave Technique

The use of microwave irradiation in the synthesis of inorganic nanomaterials represents a rather new development, although this technique is well known in organic synthetic chemistry for more than two decades.

Microwave-assisted method is one of the techniques that have been expected to be more cost-effective for large-scale production. It has increasingly been used not only because of shorter reaction time, but also uniform heating that it could provide through the entire of the reaction mixture.

Microwave provides a convenient method for studying the relationship between thermal effects and the size or shape of nanoparticles, especially when the synthesis nanosized particles.

The main advantages of this technique over conventional synthetic methods are (i) the thickness of the reaction are increased by 1-2 orders of magnitude, (ii) the initial heating process is rapid, and (iii) the microwave induce the generation of localized high temperatures at reaction sites, which enhances reaction rates.

Microwave-based synthesis are generally quite fast, simple, and very energy efficient and also show homogeneous heating characteristics.

Microwave reactors operate at a frequency of 2.45 GHz, corresponding to a photon energy of 0.0016 eV, which is too low to break chemical bonds and which is also lower than the energy of Brownian motion. Consequently, microwaves are not able to induce chemical reactions, but they offer a very efficient heating tool.

Irradiation of a reaction mixture at microwave frequencies results in alignment of the dipoles or ions in the electric field. Due to the fact that the applied field oscillates, the dipole or ion field has to realign itself continuously, which produces energy in the form of heat through molecular friction and dielectric loss.

The efficiency with which electromagnetic radiation is converted into heat is dependent on the dielectric properties of a solvent, i.e., solvents with strong ability to be polarized by the electric field are particularly advantageous for rapid heating.

Organic solvents with high microwave absorbing properties are ethylene glycol, ethanol, dimethylsulfoxide (DMSO), isopropanol or formic acid.

Solvents without a permanent dipole moment like carbon tetrachloride, benzene or dioxane are nearly microwave transparent. These solvents can be used for microwave chemistry, as long as other reagents in the reaction mixture are polar.

Polar additives like ionic liquids can be added to otherwise low-absorbing media to increase the absorbance.

Fast and efficient heating as provided by microwave irradiation bears great potential for large-scale synthesis without suffering thermal gradient effects.

The fast energy transfer directly to the reactants allows an instantaneous decomposition of nanocrystal precursors, creating highly supersaturated solutions.

By varying the microwave irradiation time and the concentration of the surfactants it was possible to obtain rare earth oxide nanostructures ranging from small spherical nuclei to short rods and extended assemblies of nanowires.

In a typical reaction, metal acetates or metal acetylacetonates were dissolved in a mixture of oleic acid and oleylamine. After irradiating in a conventional domestic microwave oven for 5 to 15 minutes, uniform nanorods, nanowires and nanoplates of M_2O_3 (M = Pr, Nd, Sm, Eu, Gd, Tb, Dy) were obtained.

The authors also performed reference experiments, however using conventional heating and they found that the resulting nanorods were significantly less uniform than those obtained under microwave irradiation.

From these findings they concluded that microwave chemistry offered better control of the morphology.

Uniform nanoparticles is synthesized by the reduction of nickel chloride by MW irradiation. Formation of Ni metal can be observed by a change in color of solution to black. The mixture was poured into porcelain beaker, and place into a microwave oven and heat until the solution turn to black color.

7. Photochemical synthesis

Photochemical synthesis of NPs is carried out by the light-induced decomposition of a metal complex or the reduction of a metal salt by photogenerated reducing agents such as solvated electrons.

The former is called photolysis and the latter radiolysis.

The formation of photographic images on a AgBr film is a familiar photolysis reaction.

Henglein, Belloni, and their coworkers have pioneered the use of photolysis and radiolysis for the preparation of nanoscale metals.

Metals such as Cd and Tl have been obtained by photolysis.

PVP-covered Au nanocrystals are produced by the reduction of HAuCl_4 in formamide by UV-irradiation.

The reaction is free radical mediated, with the radicals being generated by photodegradation of formamide. This provides a route to ion-free reduction of HAuCl_4 .

Radiolysis of Ag salts in the presence of polyphosphates produces extremely small clusters that are stable in solution for several hours.

Effective control can be exercised over the reduction process by controlling the radiation dosage.

Marandi et al. have shown that the size of CdS nanocrystals could be controlled photochemically in the reaction of CdSO_4 and $\text{Na}_2\text{S}_2\text{O}_3$.

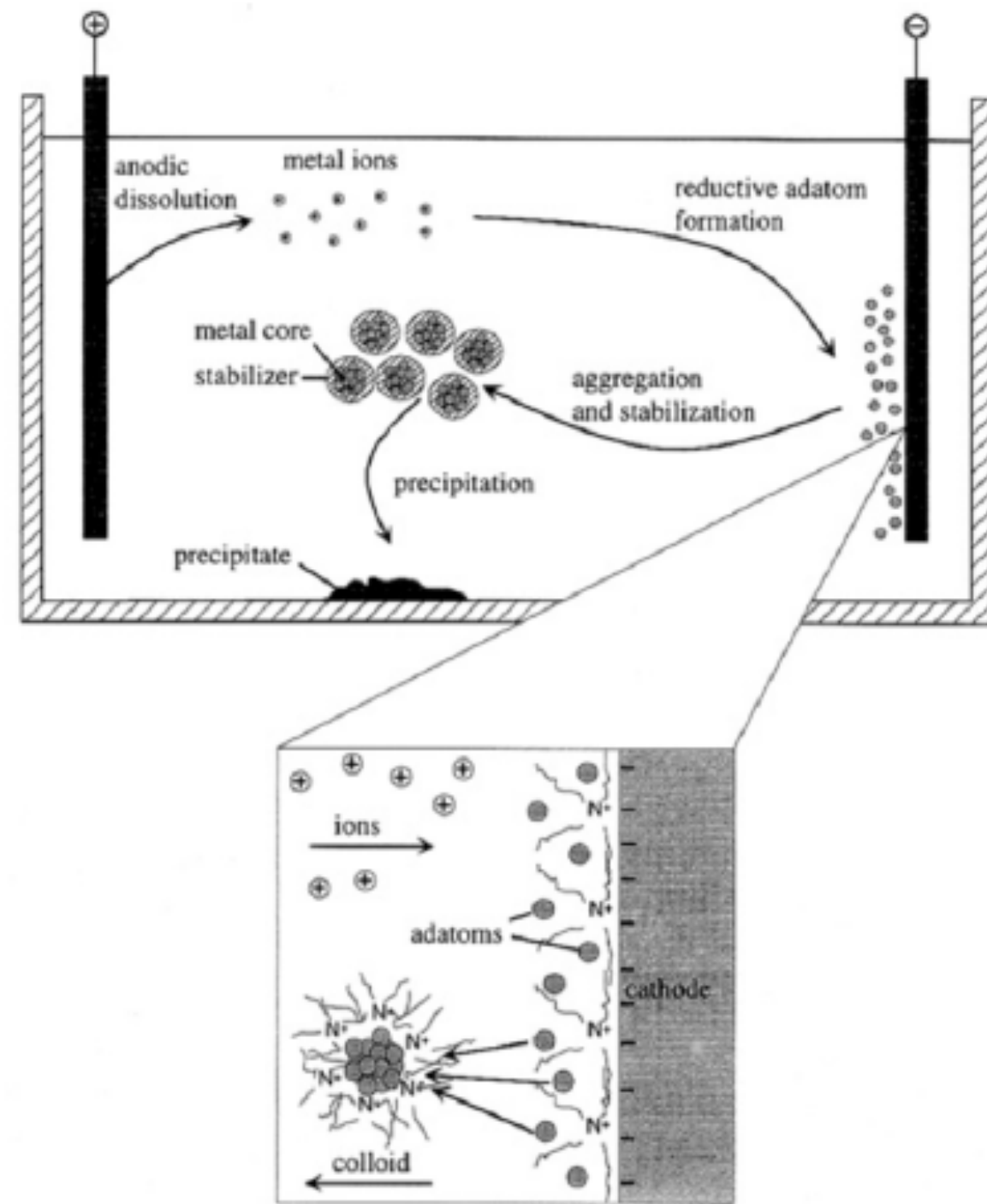
Radiolysis also provides a means for the simultaneous generation of a larger number of metal nuclei at the start of the reaction, thereby yielding a fine dispersion of nanocrystals.

8. Electrochemical synthesis

Reetz et al. have pioneered the electrochemical synthesis of metal nanocrystals.

Their method represents a refinement of the classical electro-refining process and consists of **six elementary steps** they are

- (1) oxidative dissolution of anode,
- (2) migration of metal ions to the cathodes,
- (3) reduction of ions to zero-valent state,
- (4) formation of particles by nucleation and growth,
- (5) arrest of growth by capping agents, and
- (6) precipitation of particles.



The capping agents are typically quaternary ammonium salts containing long-chain alkanes such as tetraoctylammonium bromide.

The size of the nanocrystals could be tuned by altering the current density, the distance between the electrodes, the reaction time, the temperature, and the polarity of the solvent.

Using tetraoctylammonium bromide as stabilizer, Pd nanocrystals in the size range of 1–5 nm have been obtained.

Low current densities yield larger particles (~ 4.8 nm) while large current densities yield smaller particles (~ 1.4 nm).

Larger Pd NPs stabilized by the solvent (propylene carbonate) have also been obtained. This method has been used to synthesize Ni, Co, Fe, Ti, Ag, and Au NPs.

Bimetallic colloids such as Pd–Ni, Fe–Co, and Fe–Ni have been prepared using two anodes consisting of either metals.

Mono and bimetallic particles consisting of Pt, Rh, Ru, and Mo could be prepared by reduction of their salts dissolved in the electrolyte.

Bimetallic particles could be prepared by using two ions, one of which was from the anode and the other from the metal salt dissolved in the electrolyte.

Pascal et al. synthesized maghemite ($\gamma\text{-Fe}_2\text{O}_3$) nanocrystals in the size range of 3–8 nm by the use of an Fe electrode in an aqueous solution containing DMF and cationic surfactants.

Table 2.4. Metal particles synthesized by the electrochemical reduction of salts

metal salt	<i>d</i> (nm)
PtCl ₂	2.5
PtCl ₂	5.0
RhCl ₃ H ₂ O	2.5
RuCl ₃ H ₂ O	3.5
OsCl ₃	2.0
Pd(OAc) ₂	2.5
Mo ₂ (OAc) ₄	5.0
PtCl ₂ + RuCl ₃ H ₂ O	2.5

Table 2.5. Bimetallic particles synthesized by the combination of anodic oxidation and salt reduction

anode	metal salt	<i>d</i> (nm)
Sn	PtCl ₂	3.0
Cu	Pd(OAc) ₂	2.5
Pd	PtCl ₂	3.5

9. Liquid-liquid interface synthesis

Rao and coworkers have used reactions taking place at the interface of two liquids such as toluene and water to produce nanocrystals and films of metals, semiconductors, and oxides.

In this method, a suitable organic derivative of the metal taken in the organic layer reacts at the interface with the appropriate reagent present in the aqueous layer to yield the desired product.

For example, by reacting $\text{Au}(\text{PPh}_3)\text{Cl}$ in toluene with THPC (tetrakis(hydroxymethyl)phosphonium chloride) in water, nanocrystals of Au can be obtained at the interface of two liquids, films of varying compositions.

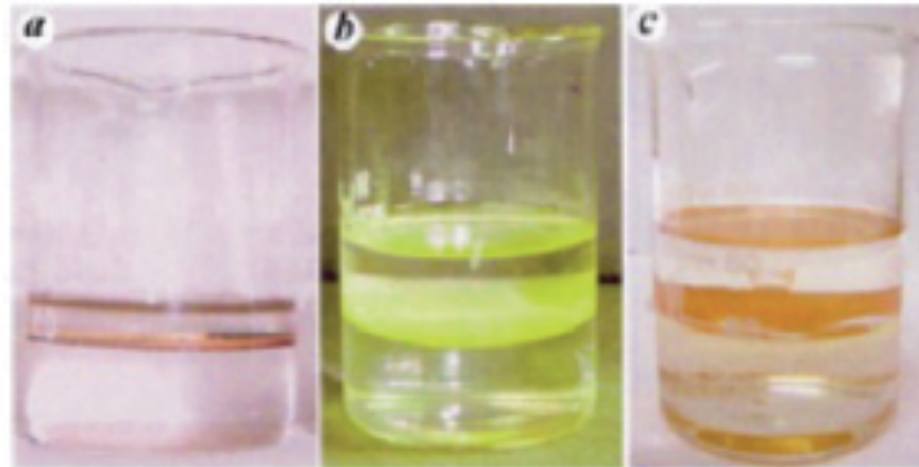


Fig. 2.17. Nanocrystals of: (a) Au, (b) CdS, and (c) $\gamma\text{-Fe}_2\text{O}_3$ formed at the toluene-water interface (reproduced with permission from [427])

This method has been extended to prepare nanocrystals of Ag and Pd, Au–Ag alloys, semiconducting sulphides such as CdS, ZnS, and CoS, and oxides such as Fe₂O₃ and CuO.

By an appropriate choice of the reaction parameters, it has been possible to obtain isolated nanocrystals with narrow size distribution or well-formed films of the nanocrystals.

By varying parameters such as the reaction temperature, and the reactant concentrations, the size of the nanocrystals and the coverage of the films can be modified.

Thus, a change in the reaction temperature from 298 to 348 K, increases the size of Au nanocrystals from 7 to 16 nm.

Starting with a mixture of metal precursors, it has been possible using this method to prepare Au–Ag alloy nanocrystalline

10. Thermolysis synthesis

Thermolysis routes are related to chemical vapor deposition (CVD)-based methods to prepare thin films.

By carrying out thermolysis reactions in high boiling solvents in the presence of capping agents, nanocrystals of various materials are obtained.

Thermal decomposition provides remarkable control over size and is well suited for scale up to gram quantities.

Various metal NPs have been prepared by decomposition of low-valent complexes involving olefinic ligands, such as cyclooctatetraene (COT), cycloocta-1,5-diene (COD), and carbonyls.

It has been known that colloidal Co can be prepared by the decomposition of Co carbonyls. Bawendi et al. carried out a similar reaction with $\text{Co}_2(\text{CO})_8$, in the presence of tri-*n*-octylphosphine oxide (TOPO) and obtained Co NPs with an average diameter of 20 nm.

By using capping agents such as carboxylic acids and alkyl amines the size of the NPs can be tuned to be in the range of 3–20 nm.

Decomposition of carbonyls has been used to prepare nanocrystals of Fe, FeCo, FeMo, FePt, CoPt, FePd, and SmCo.

Chaudret et al. have formulated a general method for the synthesis of various noble and magnetic metal NPs. The method involves the reduction of low-valent olefinic complexes with H_2 and CO.

Ag, Pt, Ru, Rh, Cu, Ir, Zn, PtRu, Co, and Ni NPs have been prepared by this method. Yase et al. have synthesized Ag NPs by the thermal decomposition of Ag carboxylates.

The reaction carried out in solid state yields capped Ag NPs dispersible in toluene.

Yase et al. have adopted this method to prepare conducting silver patterns by first screen printing with a paste consisting of Ag carboxylates.

Kim et al. have prepared Pd NPs by decomposing Pd acetate in a medium made of TOPO/TOP and oleylamine.

Nanocrystals of Cu have been obtained by thermolysis of a CVD precursor $Cu(OCH(CH_3)CH_2N(CH_3)_2)$.

Thermolytic reactions of $Pt(NH_3)_2Cl_2$ in different high boiling solvents give rise to Pt nanocrystals of complex morphologies.

Fe–Pt alloy nanocrystals with 1:1 ratio of Fe:Pt exist in two forms. An fcc (face centered cubic) form in which the Fe and Pt atoms are randomly distributed (A1 phase) or an fct (face centered tetragonal) form in which Fe and Pt layers alternate along the 001 axis (L10 phase).

The latter phase has the highest anisotropic constant among all known magnetic material.

Synthesis of homogeneously alloyed Fe–Pt nanocrystals requires that Fe and Pt are nucleated at the same time.

This process was first accomplished by reducing platinum acetylacetonate with long-chain diol and decomposing $\text{Fe}(\text{CO})_5$ in the presence of oleic acid and a long-chain amine.

There have been several improvements to the original scheme. The as-synthesized nanocrystals, present in the A1 phase, transform into the L10 phase upon annealing at 560 °C.

The transition temperature can be varied by introducing other metal ions. Thus, $[\text{Fe}_{49}\text{Pt}_{51}]$ nanocrystals have been made by introduction of silver acetylacetonate in the reaction mixture.

The A1 to L10 transition temperature is lowered to 400 °C by the introduction of Ag ions.

Cobalt and copper ions introduced in Fe–Pt nanocrystals by the cobalt acetylacetonate or copper(II) bis(2,2,6,6-tetramethyl-3,5-heptanedionate) resulted in an increase in the A1 to L10 transition temperature.

The successful synthesis of Fe–Pt nanocrystals using a combination of reduction and thermal decomposition to successfully generate homogeneous alloy nanocrystals. Thus, CoPt, FePd, and CoPt₃ have all been obtained.

Manganese–platinum alloy nanocrystals have been obtained by using platinum acetylacetonate and Mn₂(CO)₁₀ using a combination of reduction and thermal decomposition brought about using 1,2-tetradecanediol in a dioctyl ether, oleic acid/amine medium.

Ni–Fe alloy nanocrystals have been obtained using iron pentacarbonyl and Ni(C₈H₁₂)₂.

Sm–Co alloy nanocrystals have been prepared by thermolysis of Cobalt carbonyl and Samarium acetylacetonate in dioctyl ether with oleic acid.

Similarly, SmCo₅ nanocrystals have been prepared using a diol and oleic acid/amine.

Nanocrystals of metal oxides are prepared by controlled oxidation of the corresponding metal particles. Bentzon and coworkers prepared iron oxide NPs, by exposing Fe NPs, obtained by decomposing $\text{Fe}(\text{CO})_5$ in decalin in the presence of oleic acid, to air for several weeks.

By adapting a similar route, but bringing about the oxidation by using $(\text{CH}_3)_2\text{NO}$, Hyeon and coworkers have obtained $\gamma\text{-Fe}_2\text{O}_3$ NPs. The same group has extended this method to produce cobalt ferrite nanocrystals.

Alivisatos et al. prepared metal oxide NPs by the decomposition of cupferron complexes in trioctylamine solution containing octylamine. Cupferron (*N*-nitrosophenylhydroxylamine) is a versatile ligand that forms complexes with several transition metal ions.

By using this method, NPs of $\gamma\text{-Fe}_2\text{O}_3$, Cu_2O , Mn_3O_4 , Fe_3O_4 , and Co_3O_4 have been made.

The method has been used to the synthesis of nanocrystals of MnO , CoO , NiO , CuO , and ZnO .

Caprylate capped $\gamma\text{-Fe}_2\text{O}_3$ nanocrystals are obtained by the thermolysis of Fe(III) hydroxide caprylate in tetralin.

Decomposition of the acetylacetonates in hexadecylamine yields amine-capped NPs of Fe, Mn, Co, and Ni oxides.

Large Au NPs with diameters of tens of nanometers have been prepared by Nakamoto et al. by the thermolysis of Au(I) thiolate complexes.

Nanocrystals of perovskite oxides have been obtained by the thermal decomposition of MOCVD reagents (alkoxides such as $\text{BaTi}(\text{O}_2\text{CC}_7\text{H}_{15})[\text{OCH}(\text{CH}_3)_2]_5$) in diphenylether containing oleic acid and oxidizing the product with H_2O_2 . NPs of BaTiO_3 and PbTiO_3 in addition to TiO_2 are obtained by this method.

Murray et al. described a method for synthesizing CdSe nanocrystals by reacting a metal alkyl (dimethylcadmium) with TOPSe (tri-*n*-octylphosphine selenide) in TOP (tri-*n*-octylphosphine), a coordinating solvent that also acts as the capping agent.

This method readily yields CdS and CdTe nanocrystals as well.

Murray succeeds to some extent in separating the nucleation and growth steps. When the chalcogen source is injected into the hot solution, explosive nucleation occurs, accompanied by a fall in temperature. Further growth occurs by maintaining the reagents around 100 K or lower, the final size depending on the growth temperature.

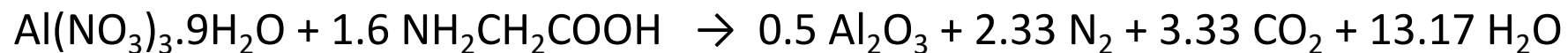
Alivisatos et al. have produced such nanocrystals by employing tri-butylphosphine at higher temperatures.

Synthesis of Al₂O₃ produced by **combustion technique**

Combustion technique is capable of producing ultrafine powders of oxide ceramics in short time at lower calcination temperature with improved powder characterization. Combustion synthesis is also known as self-propagating high-temperature synthesis (SHS).

To generate fire, an oxidizer, a fuel and the right temperature are needed. The success of the process is due to an intimate blending among the constituents using a suitable fuel or complexing agent (e.g. citric acid, urea, glycine, etc.) in an aqueous media and an exothermic redox reaction between the fuel and an oxidizer (i.e. nitrates).

The process makes use of highly exothermic redox chemical reactions between an oxidizer and a fuel. For the reaction to be self-propagating the heat evolved should be more than the heat required for initiating the combustion. Combustion process using aluminum nitrate and glycine:



Combustion synthesis is the method of choice because it is easy, safe and very fast. Hence it is energy, time saving technique and involved lower costs of preparation compared to conventional methods.

11. Biological-mediated synthesis

Of the templates and systems used for the synthesis of nanocrystals, microbes offer an interesting possibility.

The innards of a microorganism can be a tiny reactor as well as a container. Elementary reactions such as reduction are generally mediated by enzymes.

Synthesis can be carried out by simply incubating a solution of metal ions in the right microbial culture.

The ability of microbes to accumulate inorganic particles such as Au, CdS, ZnS, and magnetite is well documented in the literature.

It is also known that microorganisms put nanoscale particles to use as UV shields (CdS particles) and direction indicators (magnetite).

Nair and Pradeep have utilized *Lactobacillus* present in yogurt to synthesize Au, Ag, and Au–Ag alloy NPs. The NPs were in the size range of 15–500 nm.

Ag NPs synthesized in the size range 2-200 nm by using *Pseudomonas Stutzeri*.

Klebsiella aerogenes has been used to synthesize CdS NPs in the size range 20-200 nm.

Roh et al. have substituted metal ions such as Co, Cr, and Ni in magnetite nanocrystals synthesized using the iron-reducing bacteria *Thermoanaerobacter ethanolium*. Enzymes act as catalysts for the growth of metal NPs.

Enzyme mediated growth of metallic NPs can be exploited for various purposes in biology involving dip-pen lithography.

Apart from bacteria, yeast, and fungi have been used to obtain NPs.

Yeasts, *Candida glabrata* and *Schizosaccharomyces pombe* have been shown to yield CdS NPs.

Kowshik et al. have identified the ability of yeast *Torulopsis* sp. to produce nanoscale PbS NPs.

Sastry et al. have identified two fungi species, *Fusarium oxysporum* and *Verticillium* sp. to produce Au and Ag NPs. *Fusarium oxysporum* also reduces CdSO_4 to CdS to yield CdS NPs. CdS NPs have been produced in the extracellular space. Highly luminescent, water-soluble and biocompatible CdTe nanocrystals have been prepared by using glutathione as a stabilizer.

A novel nature of such biological synthetic is that they produce NPs at room temperature in aqueous medium, although poor size and morphology control also appear to be characteristic of these routes. Besides control over size and morphology, identification of the active biological ingredient that brings about the reaction remains unknown.

Some other synthetic methods

Synthesis of CuO nanocrystals via solid state reaction (grinding)

It is employed a general and effective approach based on one-step solid state metathesis reactions of hydrated transition metal salts and hydroxide to yield nanocrystals of oxides.

In the reaction of $\text{CuCl}_2 \cdot \text{H}_2\text{O}$ and NaOH to give CuO nanocrystals, NaCl and free water are produced and they are expected to give saturated aqueous NaCl solutions in the reaction.

The constant formation and precipitation of NaCl from the NaCl aqueous solution gives rise to NaCl “shells” surrounding the CuO particles, preventing them from aggregating to form larger size of particles.

Dissolve sodium hydroxide in distilled water and subsequently mixes with copper chloride dehydrate and ground it by using mortar and pestle.

Grind the mixtures of 45 mins. The mixture will become muddy, wash the mixture with water and EtOH , and dry in an oven.

Synthesis and characterization of nanosilica filled polypropylene composites

Two roll mill heater: a compounding method & the properties of the nanocomposites.

A two roll mill heater is melt-mixing equipment as the polymer is mixed over the softening point of the polymer.

Two roll mill heater consists of two horizontal steel rolls of the same diameter and length which lie parallel to each other with a vertical gap between them. Both rolls are capable of being heated and rotated at different speed according to the parameters needed.

Two roll milling is a method for compounding additive of fillers into thermoplastic materials and forming the thermoplastic materials into a thin sheet for subsequent molding or testing.

The polymer and fillers are subjected to high shear in the gap as the roll rotate in opposite directions.

The impact strength of the composite improve with increment of filler loading.

Thermoset composite: Preparation and characterization of silica nanoparticles filled epoxy composite

The organic compounds which contain oxirane group are known as epoxy. The commonly used epoxy resin monomers can be classified in three large groups depending on their functional groups, such as diglyceryl ether type, cycloaliphatic type and epoxy novolac resin.

Due to their ease and freedom processing, epoxy resin can be applied ranging from electronics packaging to dental applications. Common applications of epoxy composites include electronics as underfill materials in flip-chip packages and conductive adhesive, dental development, automotive, marine and aircraft applications, etc.

The hardener is used to promote the crosslink reaction. Compounds including amines, acid anhydrides and phenol-formaldehydes, have been used as curing agents.

The mechanical properties of the epoxy composite affected by the volume of filler loading.

The agglomeration of nanofiller will occur at higher filler loading.

References

Skandan, G.; Singhal, A.; Perspectives on the Science and Technology of Nanoparticle Synthesis; In *Nanomaterials Handbook*, Y. Gogotsi (Editor); Taylor & Francis: Boca Raton, 2006.

Rao, C. N. R., Thomas, P. J., Kulkarni, G. U.; *Nanocrystals: Synthesis, Properties and Application*; Springer-Verlag: Berlin, 2007.

Niederberger, M., Pinna, N.; *Metal Oxide Nanoparticles in Organic Solvents*; Springer-Verlag: London, 2009.

Aliofkhazraei, M. (Editor); *Handbook of Nanoparticles*; Springer: Switzerland, 2016.

Fecht, H. J.; Formation of Nanostructures by Mechanical Attrition; In *Nanomaterials: Synthesis, Properties and Application*, A. S. Edelstein and R. C. Cammarata (Editors); IOP Publishing: Bristol, 2001.

Koch, C. C., Top-down synthesis of nanostructured materials: mechanical and thermal processing methods, *Rev. Adv. Mater. Sci.* 2003, 5, 91-99.